Development 137, 1189-1203 (2010) doi:10.1242/dev.045732

Genomic characterization of Wilms' tumor suppressor 1 targets in nephron progenitor cells during kidney development

Sunny Hartwig[1,2], Jacqueline Ho[1,2,*], Priyanka Pandey[1,2,*], Kenzie MacIsaac[3], Mary Taglienti[1,2], Michael Xiang[4], Gil Alterovitz[4], Marco Ramoni[4], Ernest Fraenkel[3,5] and Jordan A. Kreidberg[1,2,†]

SUMMARY

The Wilms' tumor suppressor 1 (*WT1*) gene encodes a DNA- and RNA-binding protein that plays an essential role in nephron progenitor differentiation during renal development. To identify WT1 target genes that might regulate nephron progenitor differentiation in vivo, we performed chromatin immunoprecipitation (ChIP) coupled to mouse promoter microarray (ChIP-chip) using chromatin prepared from embryonic mouse kidney tissue. We identified 1663 genes bound by WT1, 86% of which contain a previously identified, conserved, high-affinity WT1 binding site. To investigate functional interactions between WT1 and candidate target genes in nephron progenitors, we used a novel, modified WT1 morpholino loss-of-function model in embryonic mouse kidney explants to knock down WT1 expression in nephron progenitors ex vivo. Low doses of WT1 morpholino resulted in reduced WT1 target gene expression specifically in nephron progenitors, whereas high doses of WT1 morpholino arrested kidney explant development and were associated with increased nephron progenitor cell apoptosis, reminiscent of the phenotype observed in *Wt1*$^{-/-}$ embryos. Collectively, our results provide a comprehensive description of endogenous WT1 target genes in nephron progenitor cells in vivo, as well as insights into the transcriptional signaling networks controlled by WT1 that might direct nephron progenitor fate during renal development.

KEY WORDS: ChIP-chip, WT1, Kidney, Progenitor, Transcription factor, Mouse

INTRODUCTION

The pediatric kidney malignancy Wilms' tumor has an incidence of 1 in 10 000 in North America (Matsunaga, 1981), making it the most common solid tumor in childhood (Bennington and Beckwith, 1975). Wilms' tumor is thought to arise from a single transformed pluripotent nephron progenitor cell whose progeny fail to undergo normal differentiation. *WT1* was the first gene identified as mutated in Wilms' tumors (Call et al., 1990; Gessler et al., 1990; Haber et al., 1990), and inactivating mutations in *Wt1* are responsible for ~10% of sporadic Wilms' tumor cases. WT1 also plays a crucial role during embryogenesis, including development of the kidneys and gonads (Kreidberg et al., 1993; Pelletier et al., 1991). At the onset of kidney development, *Wt1* is weakly expressed in the uninduced metanephric mesenchyme and increases in the cap of condensed nephrogenic progenitors surrounding the tips of the branching ureteric bud as development proceeds (Pritchard-Jones et al., 1990). Targeted mutation of *Wt1* in mice results in bilateral renal agenesis, characterized by apoptosis of the metanephric mesenchyme and failure of ureteric bud invasion into the metanephric mesenchyme (Kreidberg et al., 1993). Importantly, nephron progenitor incompetence is the primary defect in *Wt1*$^{-/-}$ embryos, as evidenced by the failure of isolated *Wt1*$^{-/-}$ mesenchymal rudiments to differentiate when co-cultured with wild-type ureteric bud cells (Donovan et al., 1999). In the complementary gain-of-function experiment, microinjection of *Wt1*-expressing plasmids into isolated embryonic kidneys stimulates nephron development (Gao et al., 2005). Collectively, these results strongly suggest that *Wt1* promotes nephron progenitor differentiation during kidney development in vivo.

Wt1 encodes a transcription factor with four Krüppel-type (Cys_2-His_2) zinc finger domains. In mammals, an alternative splice donor site at exon 9 inserts the amino acids lysine, threonine and serine (KTS) between the third and fourth zinc fingers, significantly diminishing the DNA-binding affinity of WT1 (Gessler et al., 1992; Haber et al., 1991). Thus, (+KTS) WT1 isoforms have a high affinity for RNA (Bor et al., 2006), whereas (–KTS) isoforms bind DNA with high affinity and function in transcriptional regulation. Several EGR1-like GC-rich DNA sequences and (TCC)n consensus sequences have been identified as cognate WT1 (–KTS) binding sites in vitro (Drummond et al., 1994; Rauscher et al., 1990), including a high-affinity 10-bp EGR1-like (WT1) motif (GCGTGGGCGG) associated with WT1-dependent gene transcriptional activation in vitro (Hamilton et al., 1995; Nakagama et al., 1995).

The identification of direct WT1 target genes will be essential to our understanding of WT1 function in the developing kidney and other developing organs. Therefore, to gain a deeper insight into the WT1-mediated regulatory networks that control kidney development in vivo, we initiated a systematic effort to define the genes directly regulated by WT1 during renal development. WT1-

[1]Department of Medicine, Children's Hospital Boston; Department of Pediatrics, Harvard Medical School, Boston, MA 02115, USA. [2]Harvard Stem Cell Institute, Cambridge, MA 02138, USA. [3]Department of Biological Engineering, Massachusetts Institute of Technology, Cambridge, MA 02139, USA. [4]Harvard-MIT Division of Health Sciences and Technology and Children's Hospital Informatics Program, Boston, MA 02115, USA. [5]Department of Biology and Computer Science and Artificial Intelligence Laboratory, Massachusetts Institute of Technology, Cambridge, MA 02139, USA.

*These authors contributed equally to this work
†Author for correspondence (jordan.kreidberg@childrens.harvard.edu)

Accepted 25 January 2010

directed ChIP products isolated from mouse embryonic kidneys were used to interrogate mouse promoter arrays without PCR amplification prior to hybridization, to avoid the introduction of PCR amplification bias. A large number of in vivo target sites were identified and were validated by bioinformatics analysis, ChIP-PCR, and a novel, modified WT1 morpholino loss-of-function model in embryonic kidney explants. Essential kidney development genes *Bmp7*, *Pax2* and *Sall1* were identified as WT1 transcriptional target genes and might explain the renal agenic phenotype observed in *Wt1*$^{-/-}$ embryos. Further, our data identified numerous WT1 target genes not previously studied in the developing kidney co-expressed with *Wt1* in nephron progenitors and potentially mediating its function in nephron progenitor differentiation in vivo. Collectively, these data provide novel insights into the signaling networks and biological processes that might be regulated by WT1 in nephron progenitors during kidney development in vivo.

MATERIALS AND METHODS

WT1 location analysis

Location analysis was performed as previously described (Lee et al., 2006), using pooled polyclonal anti-WT1 antibodies directed against the C-19 and N-180 terminal amino acids of WT1 (Santa Cruz), and optimized for chromatin extraction from embryonic mouse kidney tissue. Hybridization to Agilent mouse 244K promoter tiling arrays was performed using Agilent SureHyb hybridization chambers according to the manufacturer's Mammalian ChIP-on-chip v.9.0 Protocol (http://www.chem.agilent.com/Library/usermanuals/Public/G4481-90010_ManmalianProtocol_10.11.pdf) (Whitehead Institute Genome Technology Core, Cambridge, MA, USA). Raw ChIP-chip fluorescence intensity data were analyzed using ChIP Analytics 1.3.1 software (Boyer et al., 2005). Settings included spatial detrending of extracted array data, and dye-bias intra-array Lowess normalization. Normalized log-intensity and log ratio histograms followed a normal and symmetric distribution (see Fig. S1 in the supplementary material), indicating that the ChIP data are of high quality. The complete data set is available in the Array Express database (http://www.ebi.ac.uk/microarray-as/ae/, Accession No. E-TABM-872). All coordinates in this manuscript are reported in mm9.

DNA sequence motif analysis

To identify sequence motifs in WT1-bound regions detected by ChIP-chip, sequences of all 4953 WT1-bound regions were extracted and extended 200 bp from both ends. The hypothesis-driven motif discovery algorithm THEME (Macisaac et al., 2006) tested a compendium of 233 unique sequence motifs derived from ~400 mammalian transcription factor binding specificities in the TRANSFAC and JASPAR databases, to identify the enrichment of any of these motifs in WT1-bound sequences, using 5490 randomly sampled, unbound sequences for background comparison. Motifs were ranked by their mean cross-validated prediction error on held-out-bound and unbound test sequences. The top-ranking motif identified by THEME (Fig. 1A), henceforth called the WT1 matrix, comprises multiple 8-12 bp permutations of a motif consistent with the previously reported WT1 consensus sequence: GCG(T/G)(G/A)GG(C/A)G(G/T) (Hamilton et al., 1995; Nakagama et al., 1995). The statistical significance of the WT1 matrix site was determined by randomly permuting bound and unbound sequence labels and rerunning the algorithm 25 times to obtain an empirical null distribution of cross-validation errors of ~ 0.38 and an associated *z*-score of 27.5, indicating that the WT1 matrix site is highly statistically significant. To map the WT1 binding site to our bound data set, each bound region was scanned for matches to the WT1 consensus sequence, permitting the defined substitutions denoted above in the fourth, fifth, eighth and tenth positions (substitutions noted in parentheses).

Chromatin immunoprecipitation

ChIP followed by site-specific PCR (ChIP-PCR) was performed according to published protocols (Lee et al., 2006) to confirm binding of WT1 to a panel of ~ 40 WT1 target loci identified by ChIP-chip (see Table S1 in the supplementary material). Each PCR experiment comprised 5 PCR reactions: no DNA, rabbit IgG ChIP, RNA Polymerase II ChIP, WT1 ChIP and input DNA, using equimolar amounts (30 ng) of starting DNA per reaction. The following antibodies were used to perform ChIP: anti-rabbit IgG and anti-WT1 (Santa Cruz), and anti-RNA polymerase II (Upstate). The linear range of amplification was determined for each PCR reaction, with the optimal cycle number semi-quantitatively determined as 2 cycles prior to the plateau phase of amplification (see Table S2 in the supplementary material).

Wt1 vivo-morpholino treatment of embryonic kidney explants

Mouse embryonic kidneys were excised from E12.5 pregnant CD1 mice, and kidneys that had undergone 2-3 branching events were selected and transferred onto a 0.4 μM polyethylene terephthalate membrane (Falcon). Explants were cultured for 24 hours as previously described (Piscione et al., 2001), in media supplemented with either 10 μM *Wt1* antisense vivo-morpholino (5′-CAGGTCCCGCACGTCGGAACCCATG-3′) or 10 μM five-base-pair-mismatched vivo-morpholino control (5′-CAGcTCCgG CACcTCGcAACCgATG-3′) (Gene Tools).

Immunofluorescence and in situ hybridization

Immunofluorescence was performed using anti-WT1 (Santa Cruz) and anti-cytokeratin (Sigma) primary antibodies and anti-rabbit Texas Red and donkey anti-mouse FITC secondary antibodies (Jackson ImmunoResearch). TUNEL staining was performed with the Apoptag Plus Fluorescein in situ Apoptosis Detection Kit, as per manufacturer's instructions (Millipore). In situ hybridization was performed as previously described (Mo et al., 1997). The following probes were generated by PCR amplification (see Table S3 in the supplementary material) and subsequently cloned into the pCRII-TOPO vector (Invitrogen): *HeyL* (exon 5), *Cxxc5* (exon 3), *Lsp1* (5′UTR), *Pbx2* (exon 9), *Plxdc2* (5′UTR), *Rps6ka3* (exon 14-20), *Scx* (exon 1-2) and *Sox11* (3′UTR). Probes encoding *Wt1* (Gao et al., 2005), *Bmp7* (Lyons et al., 1995), *Pax2* (Dressler et al., 1990) and *Sall1* (Nishinakamura et al., 2001) have been previously described.

Quantification of apoptosis in organ explants

To quantify apoptosis, the number of TUNEL-labeled cells in the general nephron progenitor cap region was first standardized to regional surface area as previously described (Hartwig et al., 2005). This was accomplished by overlaying each digital Pax2- and TUNEL-labeled confocal image with a grid and counting the number of boxes filled by the cap region. Regional apoptosis was then quantified as the ratio of TUNEL-positive cells to the total number of filled boxes in the grid, with values presented as mean fold change in WT1-morphants versus control morphant explants (n=3). Mean differences were examined using a Student's t-test (two-tailed) and significance was taken at P<0.05.

RESULTS

Identification of loci bound by WT1

WT1 is an essential kidney development gene expressed in nephron progenitor cells that plays a crucial role in nephron progenitor differentiation in vivo. However, a comprehensive list of the transcriptional targets of WT1 that mediate its function in vivo has yet to be described. As a first step towards identifying the transcriptional targets of WT1 in nephron progenitor cells in vivo, we performed ChIP-chip on chromatin DNA isolated from embryonic mouse kidney tissue to identify genes physically bound by WT1. Chromatin immunoprecipitated with anti-WT1 antibodies (ChIP DNA) or without ChIP (input DNA) are typically amplified by PCR in order to generate sufficient DNA for hybridization to array (~10 μg DNA per channel). However, to avoid introducing bias associated with this PCR amplification step in our experiments, we processed ~1200 E18.5 kidneys, generating sufficient ChIP DNA for array hybridization without prior PCR amplification. Applying a previously published P-value cut-off of 0.001 for significant WT1 binding (Boyer et al., 2005; Lee et al., 2006), 4953 bound sequences were identified, corresponding to 1663 bound genes (see Table S4 in the supplementary material). The defined

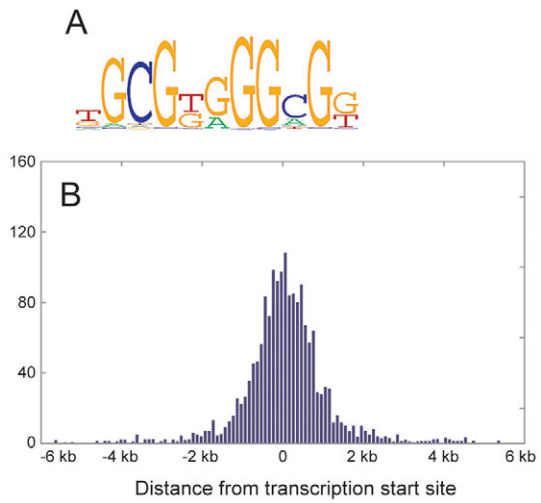

Fig. 1. Distribution of WT1 bound promoter regions and the WT1 matrix site. (**A**) Weblogo of the WT1 matrix site identified by THEME, comprising multiple permutations of a high-affinity, EGR1-like WT1 consensus site. (**B**) Histogram showing distribution of the defined peak regions of WT1-bound promoters identified by ChIP-chip in relation to the transcriptional start site (TSS). Most WT1-bound regions (~85%) and the WT1 matrix sites contained within these defined peak regions are localized within 1 kb of the TSS.

peak regions of WT1-bound promoters were largely localized (>90%) within 2 kb of the transcriptional start site (TSS; Fig. 1B). The close proximity of these cis-elements to the TSS indicate that WT1, possibly in conjunction with other co-factors, might act to stabilize general transcription factor machinery at the core promoter elements to regulate target gene transcription, as has been shown for other transcription factors that bind proximal promoter regions (Farnham, 2009).

Integrated functional annotation of WT1 target genes using DAVID knowledgebase

To interpret the biological significance of WT1 binding events in the developing kidney, we used the DAVID integrative knowledgebase (Huang da et al., 2007) to identify biological processes and molecular functions enriched in our data set. DAVID identified 64 partially overlapping functional clusters (see Table S5 in the supplementary material), which were manually organized into eight unique meta-clusters (Table 1). The most highly enriched function relates to regulation of transcription, and includes transcription factors and genes involved in chromatin establishment and modification. The second-ranking meta-cluster relates to development and differentiation in multiple tissues. In fact, *Wt1* is widely expressed in many developing organs, and *Wt1* loss-of-function mouse models have established a requirement for *Wt1* in the development of multiple organ systems, including the kidney, gonads, heart, lungs (Kreidberg et al., 1993), spleen (Herzer et al., 1999), liver (Ijpenberg et al., 2007), diaphragm (Moore et al., 1998), nervous system, vasculature (Scholz et al., 2009), brain, eye (Wagner et al., 2002), olfactory system (Wagner et al., 2005), adrenal gland and mesothelial tissues (Moore et al., 1999). The large breadth of developmental processes enriched in WT1 target genes suggests that there might indeed be a common mode of action by which WT1 regulates differentiation and development of multiple organ systems during embryogenesis. The third-ranking meta-cluster relates to cell cycle, including regulation of cell proliferation and apoptosis. The top three functional meta-clusters enriched in WT1 targets are consistent with established functions of WT1 and thus also serve as an indicator of high data set quality.

Identification of a WT1 binding motif using THEME

ChIP-chip experiments identify transcription factor binding events at low resolution. To improve the resolution of our data set, we used the THEME algorithm (Macisaac et al., 2006) to identify a sequence motif distinguishing WT1-bound target sequences from unbound sequences. The top-ranked motif identified by THEME (visualized by WebLogo in Fig. 1A and referred to as the WT1 matrix site) was detected in 86.1% of WT1-bound sites versus 34.8% of unbound sites and was consistent with the previously published EGR1-like WT1 consensus sequence (Hamilton et al., 1995; Nakagama et al., 1995). To map the WT1 binding site to our bound data set, the core WT1 consensus sequence $G^1C^2G^3(T/G)^4(G/A)^5G^6G^7(C/A)^8G^9(G/T)^{10}$ was used to scan genomic sequences, with defined substitutions permitted at the fourth, fifth, eighth or tenth positions (substitutions noted in parentheses). Notably, the WT1 consensus sequence occurs with higher frequency in higher-ranking WT1 target genes (presence of WT1 consensus site in WT1-bound promoters: 74% in genes enriched greater than 8-fold versus 25% in genes enriched less than 8-fold; $P<0.001$, Fisher's exact test). These observations indicate that high-affinity WT1 sites, as predicted by the consensus sequence, are more likely to be highly occupied in vivo. Collectively, these results indicate that the WT1 matrix site is a strong predictor of WT1 binding events in our data set.

Validation of ChIP-chip output by ChIP-PCR

To validate our ChIP-chip results by ChIP-PCR, we selected ~40 target genes from our array list that could potentially function downstream of WT1 in nephron progenitor cells (Table 2). Using both database-assisted (DAVID) annotations, as well as manual annotations (PubMed searches), targets were selected based on their established or potential roles (i.e. established role of other highly homologous family members) in kidney development, progenitor cell fate, organogenesis, cell signaling or transcriptional regulation. Targets were chosen from across a range of array enrichment scores (3- to 25-fold), to assist in determining an enrichment cut-off value for subsequent biological validation of our array data.

To verify WT1-specific enrichment of cis-regulatory regions identified by ChIP-chip, we adapted a standard ChIP protocol to perform ChIP using anti-WT1 antibodies in embryonic mouse kidney tissue (Lee et al., 2006). Following WT1 ChIP, enrichment of defined WT1-bound peak regions in ChIP fractions was compared with input fractions by PCR (see Fig. S2 in the supplementary material). A positive validation by ChIP-PCR was semi-quantitatively defined as a greater than 2-fold enrichment of WT1 ChIP DNA versus input DNA in each PCR reaction within the linear range of amplification, as measured by densitometry (NIS Elements statistical software; see Table S6 in the supplementary material). Numerous kidney development genes, including members of the Bmp (*Bmp4*, *Bmp7*, *Smad4*) and Hedgehog pathways (*Smo*, *Hhat*), as well as *Vegfa*, *Pax2* and *Sall1*, were validated as WT1 targets by ChIP-PCR (Fig. 2), suggesting that they might be bona fide transcriptional targets of WT1 in nephron progenitor cells in vivo.

Notably, lower-ranking WT1 binding sites enriched less than 8-fold on array were generally not validated by ChIP-PCR (4 were validated out of 15 ChIP-PCR reactions; see Fig. S2A-O in the supplementary material; Table 2). However, ChIP-PCR confirmed

Table 1. Functional annotation clustering of WT1 target genes using DAVID

Meta cluster		Cluster			
Rank	Term	Term	Rank	Enrichment score	Median *P*-value
1	Transcription	Transcription/regulation of transcription	1	20.43	8.64E–22
		Positive regulation (of transcription)	3	9.66	2.94E–10
		Negative regulation (of transcription)	5	7.23	1.14E–06
		Chromatin establishment/modification	24	2.39	0.002
		RNA recognition/binding	31	2.05	0.012
		(Positive) Regulation of DNA binding	59	1.45	0.047
2	Development	Development/morphogenesis/differentiation	2	16.11	2.87E–14
		Neuronal development/cellular morphogenesis	4	7.75	2.84E–07
		Regulation of development/differentiation	6	7.14	1.28E–07
		Homeobox (HOX)	9	4.84	1.38E–04
		Pattern specification	11	4.33	8.05E–05
		Skeletal development/remodeling/differentiation	12	4.06	7.18E–05
		Lung development/branching (tube) morphogenesis	13	3.88	3.90E–05
		Brain development	15	3.83	8.33E–05
		Embryonic development	16	3.83	1.07E–04
		Blood vessel development	19	2.62	0.003
		(Neural) Tube morphogenesis	20	2.55	0.004
		Muscle development/myoblast differentiation	22	2.54	0.003
		Embryonic (limb/appendage) morphogenesis	32	2.04	0.024
		Mesoderm/primary germ layer development/gastrulation	33	2	0.003
		Ear development/morphogenesis	34	2	0.010
		Embryonic digestive tract development/morphogenesis	36	1.95	0.009
		Plexin/semaphorin	38	1.79	0.013
		Gastrulation	43	1.73	0.037
		Regulation of neuron differentiation	48	1.68	0.019
		Osteoblast differentiation (regulation)	50	1.64	0.081
		Kidney/urogenital development	52	1.6	0.015
		(Positive) Regulation of axonogenesis/neurogenesis	61	1.41	0.037
		Pancreas development	63	1.35	0.032
3	Cell cycle/cell growth	Cell cycle (regulation)	7	5.49	1.92E–05
		Cell proliferation (regulation)	14	3.84	1.14E–04
		Cell growth (regulation)	21	2.55	0.003
		Apoptosis (regulation)	25	2.28	0.007
		Epithelial cell proliferation (regulation)	27	2.2	0.005
		(Negative) Regulation of cell growth	30	3.11	0.011
		Mitogen/growth factor activity	54	1.53	0.029
		Mitogen/PDGF/phosphorylation	60	1.42	0.042
4	Actin cytoskeleton	(Actin) Cytoskeleton organization and biogenesis	10	4.53	9.09E–06
		(Actin) Cytoskeleton binding	18	3.38	5.64E–04
5	DNA-binding domain/protein	Zinc finger/zinc binding	8	4.9	1.77E–05
		Basic leucine zipper (BZIP) domain	23	2.43	0.004
		(Basic) Helix-loop-helix domain/motif	29	2.14	0.012
		Dwarfin/CTF/NF-1 domain	39	1.78	0.035
		Chromatin binding/chromo domain	47	1.71	0.043
		PHD-type zinc finger domain	49	1.67	0.030
		C2H2-type zinc finger domain	53	1.55	0.118
		BTB/POZ domain	55	1.53	0.041
		Zinc finger nuclear receptors/COUP/RARA	57	1.49	0.019
6	Protein modification/kinase activity	Protein modification/phosphorylation/phosphotransferase/kinase	17	3.72	0.002
		Glycosylation/glycosyltransferase activity	26	2.25	0.006
		Golgi apparatus/glycosyltransferase activity	28	2.15	0.018
		Kinase (enzyme) binding	42	1.75	0.016
		Glycosyltransferase activity/glycan biosynthesis/manganese binding	44	1.73	0.017
		(MAPK) Phosphatase/hydrolase activity	56	1.51	0.036
		cAMP-dependent activity/cAMP binding	62	1.41	0.058
		Cation transport/channel activity	64	1.33	0.056
7	Cell adhesion/migration/signaling	(Positive) Regulation of cell migration/motility/locomotion	35	2	0.003
		Cell adhesion	37	1.86	0.015
		(Synaptic) Cell signaling	41	1.75	0.024
8	Miscellaneous protein domain	WH1/EVH1 domain	40	1.76	0.016
		GPCR/frizzled domain/PDZ binding	45	1.72	0.015
		WW domain	46	1.71	0.046
		SH3 domain	51	1.62	0.017
		Pleckstrin homology (PH) domain	58	1.48	0.100

The DAVID integrative functional annotation database identified 64 functional clusters (see Table S1 in the supplementary material) over-represented in WT1 target genes. Related clusters were manually organized into 8 major functional meta-clusters that are enriched in WT1-bound target genes.

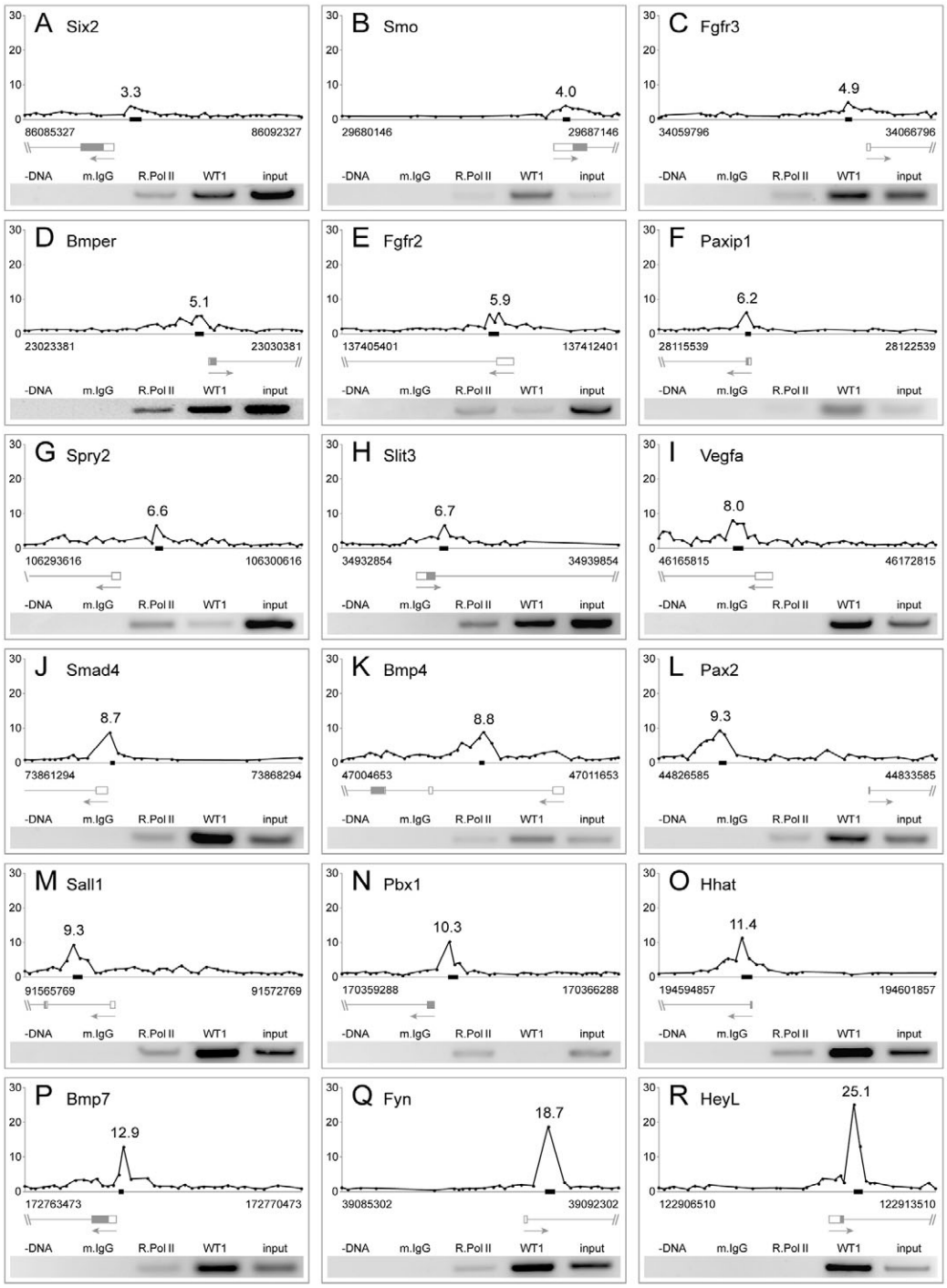

Fig. 2. ChIP-PCR validation of ChIP-chip results. (**A-R**) Plots of the mean fold-enrichment of WT1 ChIP versus input DNA (*n*=3) for selected WT1-bound genes expressed in the developing kidney. The numeric peak fold-enrichment value from the microarray is noted above the peak. The chromosomal position of the ChIP-PCR amplicon is noted along the X axis (black box). The position of the transcript is noted below the graph. The corresponding ChIP-PCR result is shown underneath. (A-H) WT1-binding sites with fold-enrichment scores less than 8-fold were generally not validated by ChIP-PCR (see Table S6 in the supplementary material for quantification of ChIP-PCR results). (I-R) By contrast, ChIP-PCR consistently confirmed WT1-specific enrichment in >90% of target genes with enrichment scores 8-fold or higher.

WT1-specific enrichment in more than 90% of higher-ranking target genes enriched greater than 8-fold (24 validated out of 26 ChIP-PCR reactions; see Fig. S2P-O′ in the supplementary material). This ChIP-PCR validation threshold of 8-fold enrichment correlates with the inflexion point of the curve identified at ~7.75-fold enrichment (R Statistical Software), when all 1663 genes were plotted against their fold-enrichment scores (see Fig. S2P′ in the supplementary material). Interestingly, among the target genes enriched greater than 8-fold, the only 2 target genes not validated by ChIP-PCR, *Pbx1* and *Pbx2* (see Fig. S2W,D′ in the supplementary material), do not

Table 2. Summary statistics of WT1 ChIP-chip peaks in selected WT1 target genes

Gene	Fold-enrichment	Chromosome	Distance to TSS	WT1 consensus site	Validated by ChIP-PCR	Function	Reference(s)
Heyl	25.11	4: 122910233-122911555	372	GCGGGGGCG	yes	*Notch* signaling pathway, cell fate determination	(Iso et al., 2003; Steidl et al., 2000)
Egr3	24.39	14: 70474926-70476048	–2009	GCGGAGGAG, GCGTGGGAGG	yes	Cellular growth and differentiation	(Tourtellotte and Milbrandt, 1998)
Actn1	23.89	12: 81360886-81361985	–193	GCGGAGGCGG, GCGGGGGAG	yes	Focal adhesion, actin cytoskeleton regulation	(Izaguirre et al., 2001)
Nab2	19.58	10: 127103344-127103263	241	GCGTGGGCG, GCGGGGG(C/A)G	yes	Schwann cell differentiation, Egr1/Egr2 co-repressor	(Le et al., 2005)
Fyn	18.7	10: 39089847-39090342	708	GCGGGGGCG	yes	Brain development, anti-apoptosis, GSD	(Arnaud et al., 2003; Harita et al., 2008; Tang et al., 2007)
Hoxd4	16.56	2: 74565721-74566423	6012	GCGGGGGCG	yes	Embryonic pattern formation, kidney development	(Di-Poi et al., 2007; reviewed in Wellick, 2009)
Sox11	15.48	12: 28027842-28028642	–657	N/A	yes	Embryonic development, neural differentiation	(Bergsland et al., 2006; Sock et al., 2004; Wurm et al., 2008)
Scx	14.68	15: 76287234-76288113	–86	GCGGGGG(C/A)GGAG	yes	Heart valve and Sertoli cell differentiation	(Levay et al., 2008; Muir et al., 2005)
Sema6d	14.11	2: 124435389-124435389	–248	GCGTGGGCGTAG	yes	Myocardial patterning	(Toyofuku et al., 2004a; Toyofuku et al., 2004b)
Bmp7	12.87	2: 172765859-172765859	–204	GCGGGGGAGGAG	yes	Eye, skeletal and kidney development	(Dudley et al., 1995; Jena et al., 1997; Kazama et al., 2008)
Pbx2	12.78	17: 34729336-34730271	252	N/A	no	Limb patterning, skeletal development	(Capellini et al., 2006; Capellini et al., 2008)
Rest	12.04	5: 77694648-77695784	–1927	GCGGGGG(C/A)G	yes	Master negative regulator of neurogenesis	(Jones and Meech, 1999; Schoenherr and Anderson, 1995)
Zfr	11.96	15: 12047157-12047853	–195	GCGGGGGAG	yes	Perigastrulation growth and survival	(Meagher et al., 2001)
Hhat	11.41	1: 194596974-194596864	219	N/A	yes	Sonic hedgehog signaling (*Shh*) pathway	(Buglino et al., 2008)
Zyx	11.38	6: 42299668-42300772	388	GCGGGGGCG	yes	Focal adhesion, cell migration, actin cytoskeleton	(Hirata et al., 2008)
Arnt2	10.9	7: 91557697-91558276	457	GCGGGGGAG	yes	Neuronal development	(Keith et al., 2001; Kozak et al., 1997)
Erbb2	10.75	11: 98273670-98274011	15	GCGGAGGAGG	yes	Neural and cardiac development, oncogene	(Lee et al., 1995)
Smad7	10.71	18: 75527141-75527426	268	GCGGAGG(C/A)GG	yes	*Tgfb*/*Bmp* signaling pathways	(Nakao et al., 1997)
Pbx1	10.27	1: 170361694-170362190	341	N/A	no	Limb patterning, skeletal and kidney development	(Capellini et al., 2006; Capellini et al., 2008; Schnabel et al., 2003)
Plxnb1	9.69	9: 108998328-109000281	1362	GCGGAGGAG	yes	Sema receptor, cell migration, invasive cell growth	(Basile et al., 2005; Giordano et al., 2002)
Pax2	9.26	19: 44827636-44828304	–3729	GCGGGGGAG	yes	Eye, inner ear and kidney development	(Rothenpieler et al., 1993; Torres et al., 1996)
Sall1	9.26	8: 91566663-91567411	1027	GCGGGGGAG	yes	Limb, neural and kidney development	(Bohm et al., 2008; Nishinakamura et al., 2001)
Bmp4	8.8	14: 47007581-47008501	2006	GCGGGGGAG	yes	Stem cell fate, kidney development	(reviewed in de Felici et al., 2009; Miyazaki et al., 2000)
Smad4	8.7	18: 73863445-73863699	–73	GCGGGGGAG	yes	*Tgfb*/*Bmp* signaling pathways	(Lagna et al., 1996; Zhang et al., 1996)
Smad3	8.16	9: 63605810-63606524	–423	GCGGGGGAGGAG, GCGGAGG(C/A)GG	yes	*Tgfb*/*Bmp* signaling pathways	(Wu, 1997; Zhang et al., 1996)
Vegfa	8.03	17: 46165927-46166243	3838	GCGTGGGCG, GCGGGGGAG	yes	Vasculogenesis, angiogenesis, kidney development	(Gao et al., 2005; Keck et al., 1989; Leung et al., 1989)

Table 2 continued on next page

contain the WT1 consensus site (Table 2). In all subsequent experiments, we therefore focused on the cohort of WT1 targets exhibiting enrichment scores greater than 8-fold by array (n=202).

WT1 morpholino treatment arrests development in embryonic kidney explants

The absence of kidneys in *Wt1*$^{-/-}$ mice has precluded conventional approaches of investigating WT1 function during early renal development in vivo. Therefore, to gain insight into the role of WT1 during early kidney development, we used a novel, modified antisense, 'vivo-morpholino' delivery system (Gene Tools) to examine the consequences of WT1 knock-down in cultured E12.5 kidney explants. Each vivo-morpholino is a fusion moiety comprising a standard morpholino covalently fused to an octaguanidium dendramer transporter at its 5′ end, permitting morpholino penetration into mouse tissue. Embryonic E12.5 mouse kidneys were cultured for 24 hours in media supplemented with WT1 antisense or 5-mismatch control vivo-morpholinos at varying dosages (10-20 μM). Anti-WT1 immunofluorescent staining was used to determine the efficacy of WT1 antisense vivo-morpholinos in blocking WT1 protein translation, and ureteric bud branching was visualized using anti-cytokeratin antibodies (Fig. 3). After 24 hours of culture, explants cultured with 10 μM control vivo-morpholino (henceforth called control morphants) had undergone extensive ureteric bud branching, similar to explants cultured in media alone (Fig. 3C,C′ versus A,A′). Control morphants exhibited characteristic WT1 expression in the cap of nephron progenitors surrounding the ureteric bud tips, as well as in pretubular aggregates, also similar to explants cultured in media alone. By contrast, WT1 expression in nephron progenitors was markedly reduced in explants treated with 10 μM WT1 vivo-morpholino (hitherto referred to as WT1 morphants; n=6; Fig. 3D,D′ versus C,C′). Decreased WT1 expression in WT1 morphants was associated with moderately reduced ureteric bud branching and overall explant size.

To examine the effects of increased WT1 morpholino concentration, we next treated explants with a high dose (20 μM) of vivo-morpholino. Control morphants treated with 20 μM control vivo-morpholino exhibited a moderate reduction in ureteric bud branch number associated with altered terminal ureteric bud tip morphology compared with explants cultured in media alone,

Table 2. Continued

Gene	Fold-enrichment	Chromosome	Distance to TSS	WT1 consensus site	Validated by ChIP-PCR	Function	Reference(s)
Nab1	7.65	1: 52556594-52556904	322	N/A	no	Schwann cell differentiation, Egr1/Egr2 co-repressor	(Le et al.,2005)
Ptch1	6.87	13: 63665972-63666429	532	GCGTGGGCG	no	*Shh* signaling pathway	(Murone et al., 1999; Stone et al., 1996)
Slit3	6.67	11: 34935290-34935979	523	GCGGAGGAG(T/G)	no	Embryonic development, kidney development	(Liu et al., 2003)
Spry2	6.6	14: 106296835-106297186	–938	N/A	no	Embryonic development, Fgf signaling	(Taniguchi et al., 2007; Taketomi et al., 2005)
PTIP	6.17	5: 28117756-28117994	101	GCGGGGGCG	yes	Cell proliferation, DNA repair, Pax2-interacting	(Cho et al., 2003)
Lef1	5.95	3: 130814332-130815403	1166	GCGGGGG(C/A)GGAG, GCGGAGGAGG	no	*Wnt* signaling pathway	(Huber et al., 1996)
Fgfr2	5.93	7: 137409139-137409581	922	GCGGGGGCG	no	Stem cell fate, kidney development	(Poladia et al., 2006; Xu et al., 1998; Zhao et al., 2004)
Sulf2	5.2	2: 165980866-165981075	262	N/A	yes	Skeletal and renal development	(Ai, et al., 2007; Holst et al., 2007)
Bmper	5.12	9: 23027603-23027893	351	N/A	no	*Bmp* signaling pathway, endothelial cell migration	(Heinke et al., 2008)
Fgfr3	4.92	5: 34064468-34064972	236	GCGGGGGCG	no	Stem cell fate, kidney development	(Poladia et al., 2006; Xu et al., 1998; Zhao et al., 2004)
Six4	4.75	12: 74213237-74213712	972	N/A	no	Neuronal cell survival, kidney induction	(Kobayashi et al., 2007; Konishi et al., 2006)
Stau1	4.52	2: 166820990-166821445	590	N/A	no	RNA-binding, embryonic stem cell differentiation	(Gautrey et al., 2008; Marion et al., 1999)
Smad6	4.34	9: 63870056-63870384	–1103	N/A	yes	*Tgfb*/*Bmp* signaling pathways	(Hata et al., 1998)
Smo	3.97	6: 29685666-29686165	328	N/A	yes	*Shh* signaling pathway	(Alcedo et al., 1996)
Six2	3.34	17: 86088110-86088338	–551	N/A	no	Stem cell self-renewal, kidney development	(Kobayashi et al., 2008; Self et al., 2006)

First tier peaks of 41 WT1 target genes identified by ChIP-chip (P< 0.001) selected for subsequent ChIP-PCR validation. Genes are ranked by fold-enrichment scores on array. Locations of defined peak regions and gene functions are noted. Negative values indicate locations upstream (5′) of the TSS. WT1 consensus sites were mapped to defined peak regions and, where present, are noted. Our WT1 consensus site mapping tolerates defined nucleotide substitutions within the 10 bp consensus sequence $G^{1}C^{2}G^{3}(T/G)^{4}(G/A)^{5}G^{6}G^{7}(C/A)^{8}G^{9}(G/T)^{10}$ identified by the motif discovery algorithm THEME, at the fourth, fifth, eighth or tenth positions (substitutions noted in parentheses). Of the 1663 WT1 target genes identified on array, the WT1 consensus site occurs with higher frequency (74%) in target genes enriched >8-fold (versus 25% in genes enriched <8-fold; P<0.0001 by Fisher's Exact Test). Among the 41 target genes selected for ChIP-PCR validation shown here, 24 of the 26 (92%) target genes enriched >8-fold were validated by ChIP-PCR as measured by >2-fold enrichment of WT1 ChIP versus input DNA using densitometry (see Fig. S2 and Table S6 in the supplementary material), of which 22 contain the WT1 consensus site. Note that the two target genes in this cohort not validated by ChIP-PCR, namely *Pbx1* and *Pbx2*, lack the WT1 consensus site. By contrast, only 4 of 15 (27%) target genes enriched <8-fold were validated by ChIP-PCR. Within the cohort of targets enriched <8-fold, there is no correlation between the presence of a WT1 consensus site and validation by ChIP-PCR. TSS, transcriptional start site; N/A, not applicable (no WT1 consensus site present). Red font denotes positive ChIP-PCR validation. Red line marks the 8-fold enrichment threshold.

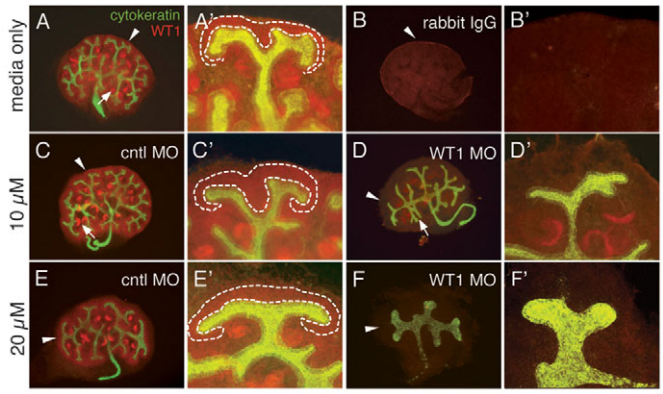

Fig. 3. Reduced WT1 expression and arrested development in WT1 morphant kidney explants. (**A**,**A′**,**C**,**C′**) E12.5 kidney explants cultured for 24 hours in media alone (A,A′) or in 10 μM control morpholino (cntl MO; C,C′) exhibit strong WT1 (red) expression in the cap of nephron progenitors (dashed outlines) surrounding the tip of the ureteric bud (green), as well as in epithelialized nephrogenic structures (arrows). Arrowheads denote regions shown in high magnification in adjacent panels. (**B**,**B′**) Background auto-fluorescence in negative control explants incubated with rabbit IgG. (**D**,**D′**) WT1 expression is markedly reduced in the cap region and moderately reduced in epithelialized nephrogenic structures of explants treated with 10 μM WT1 MO. The number of WT1-expressing nephrogenic tubules is also reduced in these explants. (**E**,**E′**) Explants treated with 20 μM cntl MO exhibit moderate reductions in ureteric bud branching compared with explants cultured in media alone but continue to express WT1 in nephron progenitor cells and form WT1-expressing epithelialized nephrogenic structures. (**F**,**F′**) By contrast, WT1 expression is not detected in explants treated with 20 μM WT1 MO, and explants do not undergo growth or ureteric bud branching.

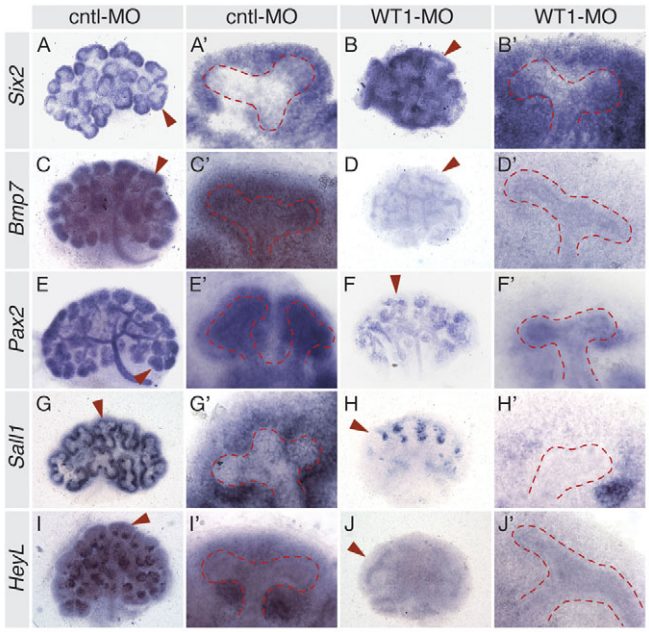

Fig. 4. Expression of kidney development WT1 target genes is reduced in WT1 morphant kidney explants. (**A**,**A′**) Control morphant explants exhibit a characteristic expression pattern of *Six2*, a marker of nephron progenitors. (A′) Higher magnification of region in A denoted by arrowhead. Dashed lines demarcate the ureteric bud. (**B**,**B′**) The discrete pattern of cap-specific *Six2* expression is lost in WT1 morphants, which instead exhibit an expanded *Six2* expression domain. (**C-J′**) Control morphants express *Bmp7* (C,C′), *Pax2* (E,E′), *Sall1* (G,G′) and *HeyL* (I,I′) in nephron progenitors and other lineages. In all cases, WT1 vivo-morpholino treatment results in a specific and marked reduction of gene expression in nephron progenitor cells (D,D′,F,F′,H,H′,J,J′). Arrowheads denote regions shown in higher magnification in adjacent panels.

indicative of a mild, general cytotoxic effect of vivo-morpholino treatment at this dosage, independent of effects on WT1 expression. Nevertheless, control morphants retained strong WT1 expression in nephron progenitors and epithelial tubules and underwent branching (Fig. 3E,E′). By contrast, WT1 expression was not detected in explants treated with 20 μM antisense WT1 vivo-morpholino, and loss of WT1 was associated with arrested ureteric bud branching and reduced overall explant size. In all subsequent experiments, 10 μM of WT1 vivo-morpholino was used, a dosage at which WT1 expression is reduced in nephron progenitors while maintaining the presence of progenitor cells.

Having demonstrated that WT1 expression is reduced in embryonic kidney explants treated with WT1 vivo-morpholinos, we proposed to use this vivo-morpholino system to examine whether WT1 target genes identified by array are indeed regulated by WT1. Loss of target gene expression in nephron progenitors of WT1 morphants could be attributable to a loss of specific regulation by WT1 or due to a general loss of progenitor cells. Therefore, we first determined whether nephron progenitor cells are still present in WT1 morphant explants. Explants were cultured for 24 hours with either 10 μM WT1 antisense or control vivo-morpholino (n=10) and *Six2* mRNA expression was assessed by RNA in situ hybridization (Fig. 4A,A′). *Six2* is a cap-specific marker of nephron progenitors surrounding ureteric bud tips (Kobayashi et al., 2008) and is downregulated in pretubular aggregates (Self et al., 2006). *Six2* was identified as a WT1 target gene (enriched 3.3-fold) by ChIP-chip. However, *Six2* was not validated by ChIP-PCR (Fig. 2A), and we therefore examined *Six2* expression in morpholino-treated explants as a negative control. Characteristically discrete *Six2* mRNA expression was detected in the cap of nephron progenitors of control morphants, tightly condensed around ureteric bud tips (Fig. 4A,A′). *Six2* expression was also detected in WT1 morphant explants (Fig. 4B,B′ versus A,A′). This was confirmed by qRT-PCR for *Six2*, which revealed no significant difference in *Six2* mRNA levels (1.1-fold higher in morphants; s.d. for WT1 morphants=0.158; s.d. for control morphants=0.136 normalized to GAPDH; n=3). However, the *Six2* expression domain appeared less compact adjacent to ureteric bud tips in these explants, possibly reflecting a failure of nephron progenitors to undergo condensation in the absence of WT1. Although we are not able to rescue WT1 expression in morpholino-treated explants, to completely eliminate the possibility of a toxic effect specific to the WT1 morpholino, the continued expression of *Six2* makes it unlikely that the WT1 morpholino is considerably more toxic than the control morpholino.

WT1 regulates expression of essential kidney development genes

Having established an ex vivo model in which to modulate WT1 expression in embryonic kidney explants while maintaining the presence of nephron progenitor cells, we next determined whether expression of essential early kidney development genes identified as WT1 targets by array are indeed regulated by WT1. In contrast to *Six2*, WT1 targets identified by array, including *Pax2* (enriched 9.3-

fold), *Sall1* (enriched 9.3-fold), *Bmp7* (enriched 12.9-fold) and *HeyL* (enriched 25.1-fold), were all validated by ChIP-PCR (Fig. 2L,M,P,R) and are regulated by WT1 (Fig. 4C-J′). In control morphants, *Bmp7* (Lyons et al., 1995) and *Pax2* (Dressler et al., 1990) mRNA expression was strongly detected in the ureteric bud and nephron progenitors and weakly expressed in pretubular aggregates (Fig. 4C,C′,E,E′). *Sall1* expression was detected predominantly in nephron progenitors and weakly in nephrogenic tubules of control morphants (Fig. 4G,G′) (Nishinakamura et al., 2001), whereas *HeyL* was expressed in nephron progenitors and ureteric bud cells (Leimeister et al., 2003), with strongest expression in pretubular aggregates (Fig. 4I,I′). In all cases, WT1 morphants exhibited a marked and specific reduction in target gene expression in nephron progenitors (Fig. 4D,D′,F,F′,H,H′,J,J′ versus C,C′,E,E′,G,G′,I,I′), whereas residual *Bmp7* and *Pax2* expression was retained in the ureteric bud.

Importantly, the demonstration that *Six2*-expressing nephron progenitor cells are indeed present in WT1 morphants (Fig. 4B,B′) indicates that loss of *Bmp7*, *Pax2*, *Sall1* and *HeyL* expression in nephron progenitors is not attributable to the absence of nephron progenitor cells. Rather, WT1-deficient nephron progenitors are present, but do not express these WT1 target genes. Collectively, these findings, which recapitulate both array and ChIP-PCR results, strongly suggest that *Bmp7*, *Pax2*, *Sall1* and *HeyL* are bona fide transcriptional targets of WT1 in embryonic kidneys. Notably, both *Pax2*$^{-/-}$ and *Sall1*$^{-/-}$ mice exhibit renal agenesis phenotypes. Our observations that these essential kidney development genes are regulated by WT1 suggest that loss of *Pax2*- and *Sall1*-dependent signaling in *Wt1*$^{-/-}$ embryos might account for the renal agenic phenotype in these embryos.

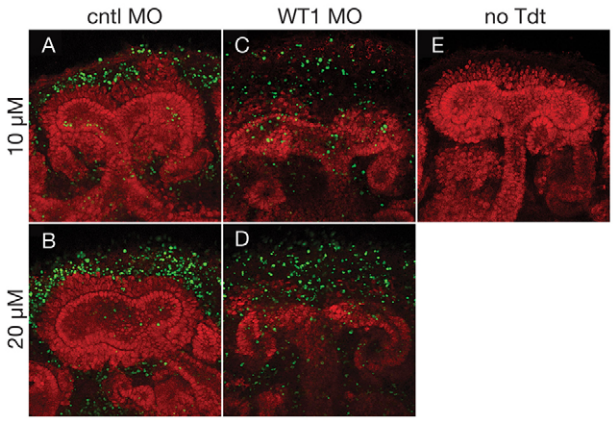

Fig. 5. Increased apoptosis in WT1 morphant explants, shown by TUNEL labeling. (**A**,**B**) Control morphant kidney explants treated with low (10 μM) or higher doses (20 μM) of control vivo-morpholino exhibit TUNEL-positive cells (green) mainly in the mesenchyme peripheral to the *Pax2* (red) expression domain of nephron progenitors and ureteric bud. (**C**,**D**) Low (C) and high (D) doses of WT1 vivo-morpholino result in an expansion of this outer apoptotic zone, which extends further in towards the centre of the explant. The number of apoptotic cells in the nephron progenitor cap region and in ureteric bud is increased in WT1 morphants (C,D versus A,B). At high doses of WT1 vivo-morpholino, a marked increase in the number of apoptotic cells is observed in the cap region adjacent to the ureteric bud (D). Note that *Pax2* expression is reduced in progenitor cells of WT1 morphant explants compared with controls (C,D versus A,B). (**E**) Negative control explant processed without Tdt enzyme showing absence of TUNEL-positivity.

Increased apoptosis in WT1 morphant kidneys

WT1 vivo-morpholino treatment of embryonic kidney explants reduces expression of essential kidney development genes *Bmp7*, *Pax2* and *Sall1*. Increased mesenchymal apoptosis is observed in *Bmp7*$^{-/-}$ (Luo et al., 1995), *Sall1*$^{-/-}$(Nishinakamura et al., 2001) and *Wt1*$^{-/-}$ embryos (Kreidberg et al., 1993) and it has been proposed that these genes might control renal development in part via anti-apoptotic effects. To determine whether apoptosis is altered in WT1 morphants, we performed TUNEL staining in WT1 morphant explants, together with Pax2 immunostaining to identify ureteric bud and nephron progenitor cells and visualized explants by confocal microscopy (Fig. 5). In explants treated with 10 or 20 μM control vivo-morpholino (Fig. 5A,B), the highest concentration of TUNEL-positive cells (green) was observed in the peripheral region of metanephric mesenchyme, with low numbers of TUNEL-positive cells also observed in the ureteric bud, nephron progenitors and stromal compartment. The number of apoptotic cells in the cap region of explants treated with 10 μM control vivo-morpholino was not significantly different from explants treated with 20 μM control vivo-morpholino (P=0.62, n=3). In WT1 morphant explants, Pax2 expression was reduced in the cap region (Fig. 5C,D), consistent with our previous results demonstrating reduced *Pax2* mRNA expression in WT1 morphant explants (Fig. 4F,F′ versus E,E′). In WT1 morphants, the peripheral apoptotic zone was expanded towards the center of the explant and a dose-dependent increase in the number of TUNEL-positive cells is observed in the cap region of nephron progenitors at ureteric bud tips. Explants treated with 10 μM WT1 vivo-morpholino exhibited a 2.5-fold increase in TUNEL-positive cells in the cap region (P=0.03) compared with explants treated with 10 μM control morpholino (Fig. 5C versus A; n=3). Explants treated with 20 μM WT1 vivo-morpholino exhibited a 4.22-fold increase in TUNEL-positive cells in the cap region (P<0.0001) compared with explants treated with 20 μM control vivo-morpholino (Fig. 5D versus B; n=3). Thus, the loss of WT1 in WT1 morphant explants is associated with reduced expression of *Bmp7*, *Pax2* and *Sall1*, together with increased apoptosis in the cap region and ureteric bud.

Novel kidney genes are transcriptional targets of WT1

In a final series of proof-of-principle experiments, we attempted to identify novel kidney development WT1 target genes from our array target list that could mediate WT1 function in nephron progenitor differentiation. Of the 202 WT1 target genes enriched greater than 8-fold, a small cohort were selected based on established or potential roles in progenitor cell fate, development, or cell-cell signaling/cell migration. In E18.5 mouse kidneys, *Wt1* expression is not restricted to nephron progenitors, but is also strongly detected in presumptive podocytes occupying the posterior portion of developing nephrons (Pritchard-Jones et al., 1990) and in mature podocytes (Mundlos et al., 1993). As we had performed ChIP-chip in E18.5 mouse kidneys, our array target list included genes expressed in nephron progenitors, induced nephrogenic structures and mature podocytes. In order to select genes specifically expressed in early renal development, we screened the mRNA expression pattern of selected genes using the Genepaint Mouse Expression Database (http://www.genepaint.org/index.html) (Alvarez-Bolado and Eichele, 2006) to further select for genes expressed in E14.5 kidneys. We thus identified a panel of WT1 target genes enriched greater than 8-fold and co-expressed with WT1 in nephron progenitors in embryonic E14.5 kidney tissues, including *Cxxc5*, *Lsp1*, *Pbx2*, *Plexdc2*, *Rps6ka3* (*Rsk2*), *Scx* and *Sox11* (Table 3).

The mRNA expression pattern of *Cxxc5* (enriched 20.9-fold), *Lsp1* (enriched 24.4-fold), *Pbx2* (enriched 12.8-fold), *Plxdc2* (enriched 10.0-fold), *Rps6ka3* (enriched 11.9-fold), *Scx* (enriched 14.7-fold) and *Sox11* (enriched 15.5-fold) in control and WT1 morphant kidney explants is shown in Fig. 6. With the exception of *Plxdc2*, strong WT1 target gene expression was detected in nephron progenitors of control morphant explants, as well as in other cell lineages (Fig. 6). The expression of *Plxd2* appeared restricted to the outer population of metanephric mesenchyme in control morphants, a more weakly *Wt1*-expressing domain, and did not appear to be expressed in cap or ureteric bud cells (Fig. 6G,G). Similar to our previous observations (Fig. 5), WT1 morphants, in all cases, exhibited marked and specific reductions in target gene expression in nephron progenitors (Fig. 6) or metanephric mesenchyme (Fig. 6H,H′ versus G,G′). Collectively, these findings illustrate the predictive quality of our array output in identifying novel kidney genes expressed in nephron progenitors of the developing kidney that might act as mediators of WT1 function in nephron progenitors in vivo.

DISCUSSION

In the present study, we performed ChIP-chip in embryonic mouse kidney tissue without PCR amplification to identify transcriptional targets of WT1 in nephron progenitor cells during renal development in vivo. Using the THEME motif discovery algorithm, a single high-affinity WT1 binding motif was identified in 86% of the WT1-bound sequences (versus 34.8% of unbound sequences) on the array (Fig. 1). Consistent with a role for WT1 in transcriptional regulation during development, biological processes most highly enriched in WT1 target genes relate to transcription as well as development and differentiation of multiple tissues (Table 1). ChIP-PCR and biological methods validated WT1 targets enriched greater than 8-fold by array, a threshold value that closely corresponds to the inflexion point (~7.75) of the fold-enrichment curve for our data set (see Fig. S2P′ in the supplementary material).

Biological validation was performed using a novel vivo-morpholino WT1 loss-of-function ex vivo model (Fig. 3-Fig.6). Embryonic kidney organ culture is a well-established model of both organogenesis in general and early kidney development in particular. WT1 vivo-morpholino treatment of embryonic kidney explants provides a powerful new biological method for validating WT1 candidate genes and characterizing both WT1 and WT1 target-gene function during renal development ex vivo. In a broader context, the core vivo-morpholino strategy should be applicable to the study of other genes that, similar to *Wt1*, exhibit early embryonic lethal organ agenesis or complex phenotypes.

Following WT1 vivo-morpholino treatment of embryonic kidney explants, RNA in situ hybridization was performed to characterize changes in renal developmental expression patterns of WT1 target genes enriched greater than 8-fold by array, including both established kidney development genes (Fig. 4), as well as genes not previously characterized in the kidney (Fig. 6). In all cases, target gene mRNA expression overlapped with the expression domain of WT1 in nephron progenitor cells and WT1 morphants uniformly exhibited decreased target gene expression in nephron progenitor cells. Collectively, these analyses suggest with considerable confidence, that WT1 target genes enriched greater than 8-fold by ChIP-chip represent bona fide WT1 transcriptional targets during renal development. Further, these results indicate a high predictive quality of our data set to identify novel WT1 target genes co-expressed with WT1 in the developing kidney that might mediate WT1 function during nephron progenitor differentiation in vivo.

Table 3. Functions associated with novel kidney WT1 target genes

Gene	Fold-enrichment	*P*-value	Function	Reference
Cxxc5	20.95	<0.001	*Bmp4*-dependent Wnt inhibition in neural stem cells	(Andersson et al., 2009)
			Myelopoietic progenitor differentiation	(Pendino et al., 2009)
			Related *Cxxc4* inhibits nuclear beta-catenin accumulation and Tcf signaling	(Hino et al., 2001; London et al., 2004)
Lsp1	24.46	<0.001	F-actin binding	(Jongstra-Bilen et al., 1992)
			Leukocyte cell migration	(Liu et al., 2005)
Pbx2	12.78	<0.001	*Pbx1*/*Pbx2* coordinately regulate limb patterning and axial skeletal development	(Capellini et al., 2006; Capellini et al., 2008)
			Related *Pbx1* regulates ureteric bud branching	(Schnabel et al., 2003)
Plxdc2	10.03	<0.001	Potential Semaphorin growth factor receptor in neural development	(Miller et al., 2007)
Rps6ka3	11.9	<0.001	Neurite differentiation	(Fischer et al., 2009)
			Fgfr3-dependent hematopoietic transformation	(Kang et al., 2007; Kang et al., 2009)
Scx	14.68	<0.001	Tendon development	(Brent et al., 2004; Edom-Vovard et al., 2002)
			Heart valve development	(Levay et al., 2008)
			Sertoli cell differentiation	(Muir et al., 2005)
Sox11	15.48	<0.001	Tissue remodeling	(Sock et al., 2004)
			Notch-, *Bmp*- and *Pax*-dependent signaling in eye development	(Wurm et al., 2008)

Established or potential biological functions associated with selected WT1 target genes enriched >8-fold, expressed in E14.5 kidneys (Genepaint Mouse Expression Database), but not previously investigated in the developing kidney.

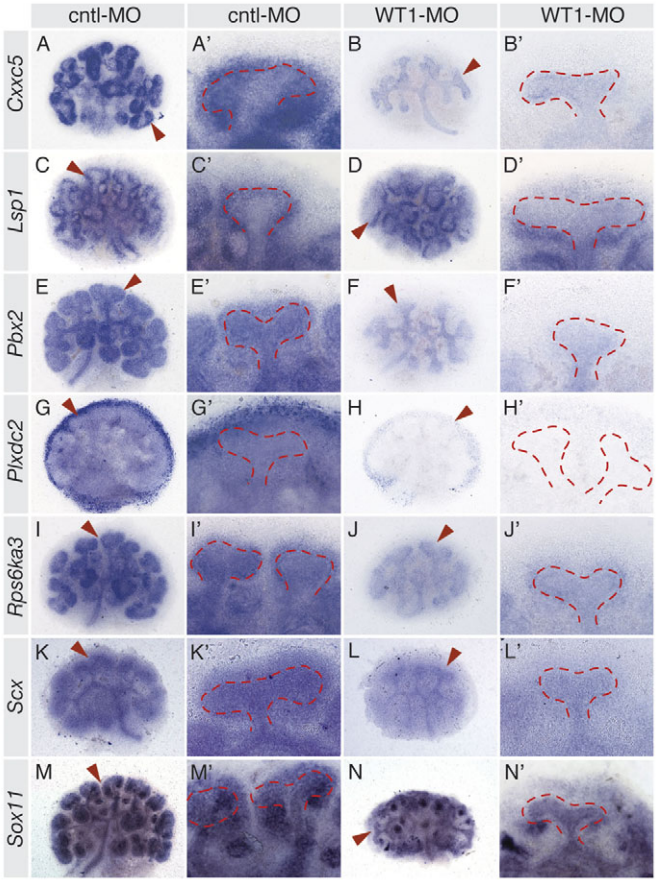

Fig. 6. Expression of novel kidney WT1 target genes is reduced in WT1 morphant kidney explants. Expression of *Cxxc5* (**A**,**A′**), *Lsp1* (**C**,**C′**), *Pbx2* (**E**,**E′**), *Rps6ka3* (**I**,**I′**), *Scx* (**K**,**K′**) and *Sox11* (**M**,**M′**) in control morphant explants, demonstrating expression in nephron progenitor cells and other lineages. *Plxdc2* (**G**,**G′**) is expressed predominantly in the outer region of the metanephric mesenchyme, a weak WT1-expression domain. In all cases, WT1 vivo-morpholino treatment results in a specific and marked reduction of target gene expression in nephron progenitor cells (**B**,**B′**,**D**,**D′**,**F**,**F′**,**J**,**J′**,**L**,**L′**,**N**,**N′**) or in mesenchyme peripheral to the nephron progenitors (**H**,**H′**). Dashed outlines demarcate the ureteric bud. Arrowheads denote regions shown in higher magnification in adjacent panels.

WT1 can function as a transcriptional activator in embryonic kidney explants

The transcriptional function of WT1 has been controversial. Primarily using promoter-reporter constructs in cell culture models of WT1 gain-of-function, WT1 has been shown to bind and repress GC-rich promoters of several growth-promoting genes expressed in the kidney including *Pax2* (Ryan et al., 1995), *N-myc* (Zhang et al., 1999) and *Egfr* (Englert et al., 1995). However, the biological relevance of many of these regulatory events is unknown, as GC-rich sequences are found in the promoter regions of thousands of genes, including those that have CpG islands. Moreover, major discrepancies were found when evaluating WT1 function using promoter-reporter constructs versus studies on the regulation of endogenous genes: in several cases, WT1 transfection failed to repress expression of the native gene, despite potently repressing the activity of its corresponding promoter-reporter constructs in transfection assays (Scharnhorst et al., 2001). For example, in the case of *Egfr*, where both endogenous gene expression and promoter activity were downregulated following WT1 transfection in Saos2 osteosarcoma cells (Englert et al., 1995), results could not be confirmed in HEK293 cells (Thate et al., 1998). Thus, WT1 transcriptional repressor activity in vitro appears to depend on promoter architecture, experimental conditions, cell line and type of expression vector (Reddy et al., 1995).

In the present study, WT1 vivo-morpholino treatment in embryonic kidney explants resulted in reduced target gene expression. These findings are consistent with the in vitro transcriptional activation function associated with the WT1 consensus site (Hamilton et al., 1995; Nakagama et al., 1995) enriched in our data set. Together with our results demonstrating physical binding of WT1 (or a WT1-containing complex) to the proximal promoter regions of these target genes, these observations indicate that WT1 can act as a transcriptional activator during embryonic renal development in vivo.

WT1 sites and target gene binding

WT1 has been shown to bind several GC-rich and (TCC)n consensus sequences in vitro (Drummond et al., 1994; Rauscher et al., 1990). In fact, the last three zinc fingers of WT1 are highly homologous with the three zinc fingers of EGR1, which each recognize a 3 bp consensus sequence. WT1 binding specificity is influenced by specific nucleotide substitutions within the core 9-bp WT1 site GCGTGGGCG in vitro. For example, adenosine and thymidine substitutions in the eighth and tenth positions (GCGTGGGAGT), respectively, have been shown to confer 20- to 30-fold higher affinity for WT1 binding compared with EGR1 in vitro (Nakagama et al., 1995). The motif discovery algorithm THEME identified a WT1 matrix site that is highly enriched in WT1-bound sequences (present in 86.1% of WT1-bound sequences versus 34.8% of unbound sequences), consistent with the previously reported, EGR1-like, WT1 consensus site (Hamilton et al., 1995; Nakagama et al., 1995). This WT1 consensus site occurs with higher frequency in higher-ranking WT1 target genes on the array (present in 74% of genes enriched greater than 8-fold versus 25% in genes enriched less than 8-fold), indicating that highly occupied in vivo WT1 targets identified by ChIP are more likely to correspond to high affinity binding sites. However, we did not observe enrichment of WT1 consensus site variants containing adenosine at the eighth position and/or thymidine at the tenth position among higher-ranking targets on the array. This might, in part, be explained by additional factors affecting recruitment of WT1 to its targets, which could include structural characteristics of the binding site that are not well-modeled by simple matrix motif models.

In addition, the observation that a significant portion (14%) of WT1-bound genes lacked the WT1 matrix site altogether, indicates that additional factors independent of cis-sequence recognition probably mediates WT1 binding to target genes in vivo. It is possible that, similar to SWI/SWF-DNA- (Fairall et al., 1993; Schwabe et al., 1993) and GLI-DNA-binding events (Pavletich and Pabo, 1993; Vokes et al., 2007), WT1 zinc finger-DNA interactions might involve a combination of cis and trans DNA-binding sequences. In addition, cooperative or competitive interactions with other transcription factors, histone modifications and the chromatin structure in the vicinity of the binding site probably play an important role in bringing WT1 to its target site and increasing WT1 binding affinity in vivo.

Functional annotations associated with WT1

DAVID identified eight major functional groups enriched in WT1 targets (Table 1). The three most enriched functions relate to transcription, multi-organ development and cell cycle, terms consistent with the established role of WT1 during development and in tumor biology. WT1 targets are also enriched for specific families of proteins containing conserved zinc-finger DNA-binding motifs including BZIP, BHLH, Dwarfin/CTF/NF-1, Chromo, PhD, C_2H_2 and BTP/POZ domains, as well as zinc-finger families of nuclear receptors. Non-DNA-binding protein domains including WH1/EVH1, GPCR, Frz/PDZ, WW, SH3 and pleckstrin homology domains were also enriched in WT1 target genes. That WT1 binds conserved families of proteins suggests a model wherein WT1-dependent transcriptional regulation of a small number of ancestral genes might have been retained following gene duplication events, chromosomal segregation, and other genome reorganization events that both increased gene number and diversified gene function during evolution (Pal and Hurst, 2000).

Interestingly, WT1 target genes were also enriched for actin cytoskeleton organization, actin biogenesis and binding, as well as cell adhesion, cell migration and cell-cell signaling. In fact, three of the top ten most highly enriched WT1 targets identified by array (see Table S4 in the supplementary material), namely *Myo1B* (enriched 27.2-fold), *Lsp1* (enriched 24.5-fold) and *Actn1* (enriched 23.8-fold), are expressed during early kidney development and are involved in cytoskeletal interactions. Previously, two independent transcriptome profiling reports during pre-implantation mouse development demonstrated an obligate, transient surge in expression of genes involved in actin cytoskeleton and cell-cell signaling occurring prior to the major differentiation events in early development (Hamatani et al., 2004; Mitiku and Baker, 2007). High expression of cytoskeleton-interacting genes at this juncture is thought to relate to the dramatic morphological changes and energy requirements associated with compaction, as well as the requirement of cadherin-cytoskeleton interactions for cell-to-cell contact and adhesion during compaction (Hamatani et al., 2006). Expression of cell-cell signaling genes is thought to facilitate assembly of gap and tight junctions that enable blastomeres to lose their round shape, become tightly packed together and undergo differentiation (Watson and Barcroft, 2001).

It is intriguing to hypothesize that a similar burst of expression of genes involved in cytoskeleton and cell-cell signaling might necessarily precede the major morphologic changes associated with nephron progenitor aggregation around ureteric bud tips and differentiation. In fact, isolated *Wt1*$^{-/-}$ mesenchymal rudiments fail to aggregate in response to inductive signals from wild-type ureteric bud cells and instead undergo massive apoptosis (Donovan et al., 1999). This phenotype is distinct from *Sall1*$^{-/-}$ rudiments, which retain their competence to respond to inducing ureteric bud signals (Nishinakamura et al., 2001), suggesting that the *Wt1*$^{-/-}$ phenotype is not simply due to loss of *Sall1* signaling. Similarly, in WT1 morphant kidney explants, WT1-deficient nephron progenitor cells fail to become tightly packed into a discrete 'cap' around the tips of the ureteric bud. Instead, WT1-deficient nephron progenitors are loosely arranged around the ureteric bud tips, as evidenced by a diffuse rather than cap-specific expression pattern of the nephron progenitor marker *Six2* (Fig. 4B,B′ versus A,A′). It is possible that one function of WT1 during early renal development is to activate genes involved in cytoskeletal-interactions, cell-cell adhesion, migration and signaling, processes that might themselves play pivotal permissive roles in nephron progenitor differentiation. In this paradigm, loss of WT1-dependent activation of cytoskeleton-interacting genes in *Wt1*$^{-/-}$ mice would reduce the cellular integrity and scaffolding of individual nephron progenitor cells, thus rendering them incompetent to withstand the major morphologic changes associated with aggregation and differentiation. Similarly, loss of WT1-dependent activation of cell-cell signaling genes might prevent groups of *Wt1*$^{-/-}$ nephron progenitor cells from forming necessary cell-cell contacts. Thus, these cells would be unable to aggregate and undergo concerted group movement to form the cap of cells that surround the ureteric bud tips and undergo differentiation.

Recently, ChIP-chip location analysis was performed in immortalized CCG099-11 Wilms' tumor cells (Kim et al., 2009) and eight WT1 target genes were initially identified in three technical replicates. By overexpressing WT1 in inducible CCG-5.1 cells, the authors subsequently identified 643 promoter targets of WT1. The highest functional enrichment in WT1 target genes related to MAPK signaling, regulation of actin cytoskeleton and focal adhesion functional groups that were also observed in our data set, albeit at the lower range of enrichment. Major differences between this data set and our own might reflect differences in WT1-dependent tumor biology versus developmental function, as well as differences obtained by performing ChIP-chip in WT1-overexpressing immortalized cells versus in embryonic kidney tissues.

During renal development, WT1 is expressed in multiple nephrogenic compartments including the nephrogenic mesenchyme, nephron progenitors and developing tubules, as well as in glomerular podocytes. Whether WT1 regulates similar sets of gene targets in each of these cellular compartments, and at different stages of renal development, has not been explored. Recently, Brunskill et al. (Brunskill et al., 2008) have used laser capture microdissection and/or fluorescence-activated cell sorting followed by microarray profiling, to define a genome-wide gene expression atlas for the different cell lineages of the developing kidney at both late and early developmental time points (Brunskill et al., 2008). The integration of our WT1 ChIP-chip results with results from the kidney atlas and other gene expression databases will be a necessary and important first step towards a comprehensive description of WT1 function and gene targets at different stages of renal development in vivo.

In summary, by applying location analysis together with bioinformatics and biological approaches, we have identified WT1 target genes in embryonic mouse kidneys co-expressed with WT1 in nephron progenitor cells that could play an important role in mediating WT1 regulation of nephron progenitor differentiation in vivo. These data provide novel insights into biological processes that might be regulated by WT1, as well as the mechanisms by which WT1 binds and regulates target gene transcription in progenitor cells of the developing kidney and other developing organs in vivo.

Acknowledgements

Dr Kreidberg's laboratory is supported by the NIDDK (R01DK070901), the Joanne Webb Fund and the Harvard Stem Cell Institute. Sunny Hartwig is the recipient of a KRESCENT fellowship. The Pax2 antibody was a gift from Dr Gregory Dressler (University of Michigan). The authors acknowledge valuable discussions with members of the Kreidberg Laboratory. Deposited in PMC for release after 12 months.

Competing interests statement

The authors declare no competing financial interests.

Supplementary material

Supplementary material for this article is available at
http://dev.biologists.org/lookup/suppl/doi:10.1242/dev.045732/-/DC1

References

Ai, X., Kitazawa, T., Do, A. T., Kusche-Gullberg, M., Labosky, P. A. and Emerson, C. P., Jr (2007). SULF1 and SULF2 regulate heparan sulfate-mediated GDNF signaling for esophageal innervation. *Development* **134**, 3327-3338.

Alcedo, J., Ayzenzon, M., Von Ohlen, T., Noll, M. and Hooper, J. E. (1996). The Drosophila smoothened gene encodes a seven-pass membrane protein, a putative receptor for the hedgehog signal. *Cell* **86**, 221-232.

Alvarez-Bolado, G. and Eichele, G. (2006). Analysing the developing brain transcriptome with the GenePaint platform. *J. Physiol.* **575**, 347-352.

Andersson, T., Sodersten, E., Duckworth, J. K., Cascante, A., Fritz, N., Sacchetti, P., Cervenka, I., Bryja, V. and Hermanson, O. (2009). CXXC5 is a novel BMP4-regulated modulator of Wnt signaling in neural stem cells. *J. Biol. Chem.* **284**, 3672-3681.

Arnaud, L., Ballif, B. A., Forster, E. and Cooper, J. A. (2003). Fyn tyrosine kinase is a critical regulator of disabled-1 during brain development. *Curr. Biol.* **13**, 9-17.

Basile, J. R., Afkhami, T. and Gutkind, J. S. (2005). Semaphorin 4D/plexin-B1 induces endothelial cell migration through the activation of PYK2, Src, and the phosphatidylinositol 3-kinase-Akt pathway. *Mol. Cell. Biol.* **25**, 6889-6898.

Bennington, J. and Beckwith, J. (1975). *Tumors of the Kidney, Renal Pelvis and Ureter.* Washington, DC: Armed Forces Institute of Pathology.

Bergsland, M. W. M., Malewicz, M., Perlmann, T. and Muhr, J. (2006). The establishment of neuronal properties is controlled by Sox4 and Sox11. *Genes Dev.* **20**, 3475-3486.

Bohm, J., Buck, A., Borozdin, W., Mannan, A. U., Matysiak-Scholze, U., Adham, I., Schulz-Schaeffer, W., Floss, T., Wurst, W., Kohlhase, J. et al. (2008). Sall1, sall2, and sall4 are required for neural tube closure in mice. *Am. J. Pathol.* **173**, 1455-1463.

Bor, Y., Swartz, J., Morrison, A., Rekosh, D., Ladomery, M. and Hammarskjold, M. L. (2006). The Wilms' tumor 1 (WT1) gene (+KTS isoform) functions with a CTE to enhance translation from an unspliced RNA with a retained intron. *Genes Dev.* **20**, 1597-1608.

Boyer, L. A., Lee, T. I., Cole, M. F., Johnstone, S. E., Levine, S. S., Zucker, J. P., Guenther, M. G., Kumar, R. M., Murray, H. L., Jenner, R. G. et al. (2005). Core transcriptional regulatory circuitry in human embryonic stem cells. *Cell* **122**, 947-956.

Brent, A. E. and Tabin, C. J. (2004). FGF acts directly on the somitic tendon progenitors through the Ets transcription factors Pea3 and Erm to regulate scleraxis expression. *Development* **131**, 3885-3896.

Brunskill, E. W., Aronow, B. J., Georgas, K., Rumballe, B., Valerius, M. T., Aronow, J., Kaimal, V., Jegga, A. G., Yu, J., Grimmond, S. et al. (2008). Atlas of gene expression in the developing kidney at microanatomic resolution. *Dev. Cell* **15**, 781-791.

Buglino, J. A. and Resh, M. D. (2008). Hhat is a palmitoylacyltransferase with specificity for N-palmitoylation of Sonic Hedgehog. *J. Biol. Chem.* **283**, 22076-22088.

Call, K. M., Glaser, T., Ito, C. Y., Buckler, A. J., Pelletier, J., Haber, D. A., Rose, E. A., Kral, A., Yeger, H., Lewis, W. H. et al. (1990). Isolation and characterization of a zinc finger polypeptide gene at the human chromosome 11 Wilms' tumor locus. *Cell* **60**, 509-520.

Capellini, T. D., Di Giacomo, G., Salsi, V., Brendolan, A., Ferretti, E., Srivastava, D., Zappavigna, V. and Selleri, L. (2006). Pbx1/Pbx2 requirement for distal limb patterning is mediated by the hierarchical control of Hox gene spatial distribution and Shh expression. *Development* **133**, 2263-2273.

Capellini, T. D., Zewdu, R., Di Giacomo, G., Asciutti, S., Kugler, J. E., Di Gregorio, A. and Selleri, L. (2008). Pbx1/Pbx2 govern axial skeletal development by controlling Polycomb and Hox in mesoderm and Pax1/Pax9 in sclerotome. *Dev. Biol.* **321**, 500-514.

Cho, E. A., Prindle, M. J. and Dressler, G. R. (2003). BRCT domain-containing protein PTIP is essential for progression through mitosis. *Mol. Cell. Biol.* **23**, 1666-1673.

De Felici, M., Farini, D. and Dolci, S. (2009). In or out stemness: comparing growth factor signalling in mouse embryonic stem cells and primordial germ cells. *Curr. Stem Cell Res. Ther.* **4**, 87-97.

Di-Poi, N., Zakany, J. and Duboule, D. (2007). Distinct roles and regulations for HoxD genes in metanephric kidney development. *PLoS Genet.* **3**, e232.

Donovan, M. J., Natoli, T. A., Sainio, K., Amstutz, A., Jaenisch, R., Sariola, H. and Kreidberg, J. A. (1999). Initial differentiation of the metanephric mesenchyme is independent of WT1 and the ureteric bud. *Dev. Genet.* **24**, 252-262.

Dressler, G. R., Deutsch, U., Chowdhury, K., Nornes, H. O. and Gruss, P. (1990). Pax2, a new murine paired-box-containing gene and its expression in the developing excretory system. *Development* **109**, 787-795.

Drummond, I. A., Rupprecht, H. D., Rohwer-Nutter, P., Lopez-Guisa, J. M., Madden, S. L., Rauscher, F. J., 3rd and Sukhatme, V. P. (1994). DNA recognition by splicing variants of the Wilms' tumor suppressor, WT1. *Mol. Cell. Biol.* **14**, 3800-3809.

Dudley, A. T., Lyons, K. M. and Robertson, E. J. (1995). A requirement for bone morphogenetic protein-7 during development of the mammalian kidney and eye. *Genes Dev.* **9**, 2795-2807.

Edom-Vovard, F., Schuler, B., Bonnin, M. A., Teillet, M. A. and Duprez, D. (2002). Fgf4 positively regulates scleraxis and tenascin expression in chick limb tendons. *Dev. Biol.* **247**, 351-366.

Englert, C., Hou, X., Maheswaran, S., Bennett, P., Ngwu, C., Re, G. G., Garvin, A. J., Rosner, M. R. and Haber, D. A. (1995). WT1 suppresses synthesis of the epidermal growth factor receptor and induces apoptosis. *EMBO J.* **14**, 4662-4675.

Fairall, L., Schwabe, J. W., Chapman, L., Finch, J. T. and Rhodes, D. (1993). The crystal structure of a two zinc-finger peptide reveals an extension to the rules for zinc-finger/DNA recognition. *Nature* **366,** 483-487.

Farnham, P. J. (2009). Insights from genomic profiling of transcription factors. *Nat. Rev. Genet.* **10**, 605-616.

Fischer, M., Pereira, P. M., Holtmann, B., Simon, C. M., Hanauer, A., Heisenberg, M. and Sendtner, M. (2009). P90 Ribosomal s6 kinase 2 negatively regulates axon growth in motoneurons. *Mol. Cell. Neurosci.* **42**, 134-141.

Gao, X., Chen, X., Taglienti, M., Rumballe, B., Little, M. H. and Kreidberg, J. A. (2005). Angioblast-mesenchyme induction of early kidney development is mediated by Wt1 and Vegfa. *Development* **132**, 5437-5449.

Gautrey, H., McConnell, J., Lako, M., Hall, J. and Hesketh, J. (2008). Staufen1 is expressed in preimplantation mouse embryos and is required for embryonic stem cell differentiation. *Biochim. Biophys. Acta* **1783**, 1935-1942.

Gessler, M., Poustka, A., Cavenee, W., Neve, R. L., Orkin, S. H. and Bruns, G. A. (1990). Homozygous deletion in Wilms tumours of a zinc-finger gene identified by chromosome jumping. *Nature* **343**, 774-778.

Gessler, M., Konig, A. and Bruns, G. A. (1992). The genomic organization and expression of the WT1 gene. *Genomics* **12**, 807-813.

Giordano, S., Corso, S., Conrotto, P., Artigiani, S., Gilestro, G., Barberis, D., Tamagnone, L. and Comoglio, P. M. (2002). The semaphorin 4D receptor controls invasive growth by coupling with Met. *Nat. Cell Biol.* **4**, 720-724.

Haber, D. A., Buckler, A. J., Glaser, T., Call, K. M., Pelletier, J., Sohn, R. L., Douglass, E. C. and Housman, D. E. (1990). An internal deletion within an 11p13 zinc finger gene contributes to the development of Wilms' tumor. *Cell* **61**, 1257-1269.

Haber, D. A., Sohn, R. L., Buckler, A. J., Pelletier, J., Call, K. M. and Housman, D. E. (1991). Alternative splicing and genomic structure of the Wilms tumor gene WT1. *Proc. Natl. Acad. Sci. USA* **88**, 9618-9622.

Hamatani, T., Carter, M. G., Sharov, A. A. and Ko, M. S. (2004). Dynamics of global gene expression changes during mouse preimplantation development. *Dev. Cell* **6**, 117-131.

Hamatani, T., Ko, M., Yamada, M., Kuji, N., Mizusawa, Y., Shoji, M., Hada, T., Asada, H., Maruyama, T. and Yoshimura, Y. (2006). Global gene expression profiling of preimplantation embryos. *Hum. Cell* **19**, 98-117.

Hamilton, T. B., Barilla, K. C. and Romaniuk, P. J. (1995). High affinity binding sites for the Wilms' tumour suppressor protein WT1. *Nucleic Acids Res.* **23**, 277-284.

Harita, Y., Kurihara, H., Kosako, H., Tezuka, T., Sekine, T., Igarashi, T. and Hattori, S. (2008). Neph1, a component of the kidney slit diaphragm, is tyrosine-phosphorylated by the Src family tyrosine kinase and modulates intracellular signaling by binding to Grb2. *J. Biol. Chem.* **283**, 9177-9186.

Hartwig, S., Hu, M. C., Cella, C., Piscione, T., Filmus, J. and Rosenblum, N. D. (2005). Glypican-3 modulates inhibitory Bmp2-Smad signaling to control renal development in vivo. *Mech. Dev.* **122,** 928-38.

Hata, A., Lagna, G., Massague, J. and Hemmati-Brivanlou, A. (1998). Smad6 inhibits BMP/Smad1 signaling by specifically competing with the Smad4 tumor suppressor. *Genes Dev.* **12**, 186-197.

Heinke, J., Wehofsits, L., Zhou, Q., Zoeller, C., Baar, K. M., Helbing, T., Laib, A., Augustin, H., Bode, C., Patterson, C. et al. (2008). BMPER is an endothelial cell regulator and controls bone morphogenetic protein-4-dependent angiogenesis. *Circ. Res.* **103**, 804-812.

Herzer, U., Crocoll, A., Barton, D., Howells, N. and Englert, C. (1999). The Wilms tumor suppressor gene wt1 is required for development of the spleen. *Curr. Biol.* **9**, 837-840.

Hino, S., Kishida, S., Michiue, T., Fukui, A., Sakamoto, I., Takada, S., Asashima, M. and Kikuchi, A. (2001). Inhibition of the Wnt signaling pathway by Idax, a novel Dvl-binding protein. *Mol. Cell. Biol.* **21**, 330-342.

Holst, C. R., Bou-Reslan, H., Gore, B. B., Wong, K., Grant, D., Chalasani, S., Carano, R. A., Frantz, G. D., Tessier-Lavigne, M., Bolon, B. et al. (2007). Secreted sulfatases Sulf1 and Sulf2 have overlapping yet essential roles in mouse neonatal survival. *PLoS One* **2**, e575.

Huang da, W., Sherman, B. T., Tan, Q., Collins, J. R., Alvord, W. G., Roayaei, J., Stephens, R., Baseler, M. W., Lane, H. C. and Lempicki, R. A. (2007). The DAVID Gene Functional Classification Tool: a novel biological module-centric algorithm to functionally analyze large gene lists. *Genome Biol.* **8**, R183.

Huber, O., Korn, R., McLaughlin, J., Ohsugi, M., Herrmann, B. G. and Kemler, R. (1996). Nuclear localization of beta-catenin by interaction with transcription factor LEF-1. *Mech. Dev.* **59**, 3-10.

Ijpenberg, A., Perez-Pomares, J. M., Guadix, J. A., Carmona, R., Portillo-Sanchez, V., Macias, D., Hohenstein, P., Miles, C. M., Hastie, N. D. and Munoz-Chapuli, R. (2007). Wt1 and retinoic acid signaling are essential for stellate cell development and liver morphogenesis. *Dev. Biol.* **312**, 157-170.

Iso, T., Kedes, L. and Hamamori, Y. (2003). HES and HERP families: multiple effectors of the Notch signaling pathway. *J. Cell. Physiol.* **194**, 237-255.
Izaguirre, G., Aguirre, L., Hu, Y. P., Lee, H. Y., Schlaepfer, D. D., Aneskievich, B. J. and Haimovich, B. (2001). The cytoskeletal/non-muscle isoform of alpha-actinin is phosphorylated on its actin-binding domain by the focal adhesion kinase. *J. Biol. Chem.* **276**, 28676-28685.
Jena, N., Martin-Seisdedos, C., McCue, P. and Croce, C. M. (1997). BMP7 null mutation in mice: developmental defects in skeleton, kidney, and eye. *Exp. Cell Res.* **230**, 28-37.
Jongstra-Bilen, J., Janmey, P. A., Hartwig, J. H., Galea, S. and Jongstra, J. (1992). The lymphocyte-specific protein LSP1 binds to F-actin and to the cytoskeleton through its COOH-terminal basic domain. *J. Cell Biol.* **118**, 1443-1453.
Kang, S., Dong, S., Gu, T. L., Guo, A., Cohen, M. S., Lonial, S., Khoury, H. J., Fabbro, D., Gilliland, D. G., Bergsagel, P. L. et al. (2007). FGFR3 activates RSK2 to mediate hematopoietic transformation through tyrosine phosphorylation of RSK2 and activation of the MEK/ERK pathway. *Cancer Cell* **12**, 201-214.
Kang, S., Elf, S., Dong, S., Hitosugi, T., Lythgoe, K., Guo, A., Ruan, H., Lonial, S., Khoury, H. J., Williams, I. R. et al. (2009). Fibroblast growth factor receptor 3 associates with and tyrosine phosphorylates p90 RSK2, leading to RSK2 activation that mediates hematopoietic transformation. *Mol. Cell. Biol.* **29**, 2105-2117.
Kazama, I., Mahoney, Z., Miner, J. H., Graf, D., Economides, A. N. and Kreidberg, J. A. (2008). Podocyte-derived BMP7 is critical for nephron development. *J. Am. Soc. Nephrol.* **19**, 2181-2191.
Keck, P. J., Hauser, S. D., Krivi, G., Sanzo, K., Warren, T., Feder, J. and Connolly, D. T. (1989). Vascular permeability factor, an endothelial cell mitogen related to PDGF. *Science* **246**, 1309-1312.
Keith, B., Adelman, D. M. and Simon, M. C. (2001). Targeted mutation of the murine arylhydrocarbon receptor nuclear translocator 2 (Arnt2) gene reveals partial redundancy with Arnt. *Proc. Natl. Acad. Sci. USA* **98**, 6692-6697.
Kim, M. K., McGarry, T. J., O Broin, P., Flatow, J. M., Golden, A. A. and Licht, J. D. (2009). An integrated genome screen identifies the Wnt signaling pathway as a major target of WT1. *Proc. Natl. Acad. Sci. USA* **106**, 11154-11159.
Kobayashi, H., Kawakami, K., Asashima, M. and Nishinakamura, R. (2007). Six1 and Six4 are essential for Gdnf expression in the metanephric mesenchyme and ureteric bud formation, while Six1 deficiency alone causes mesonephric-tubule defects. *Mech. Dev.* **124**, 290-303.
Kobayashi, A., Valerius, M. T., Mugford, J. W., Carroll, T. J., Self, M., Oliver, G. and McMahon, A. P. (2008). Six2 defines and regulates a multipotent self-renewing nephron progenitor population throughout mammalian kidney development. *Cell Stem Cell* **3**, 169-181.
Konishi, Y., Ikeda, K., Iwakura, Y. and Kawakami, K. (2006). Six1 and Six4 promote survival of sensory neurons during early trigeminal gangliogenesis. *Brain Res.* **1116**, 93-102.
Kozak, K. R., Abbott, B. and Hankinson, O. (1997). ARNT-deficient mice and placental differentiation. *Dev. Biol.* **191**, 297-305.
Kreidberg, J. A., Sariola, H., Loring, J. M., Maeda, M., Pelletier, J., Housman, D. and Jaenisch, R. (1993). WT-1 is required for early kidney development. *Cell* **74**, 679-691.
Lagna, G., Hata, A., Hemmati-Brivanlou, A. and Massague, J. (1996). Partnership between DPC4 and SMAD proteins in TGF-beta signalling pathways. *Nature* **383**, 832-836.
Le, N., Nagarajan, R., Wang, J. Y., Svaren, J., LaPash, C., Araki, T., Schmidt, R. E. and Milbrandt, J. (2005). Nab proteins are essential for peripheral nervous system myelination. *Nat. Neurosci.* **8**, 932-940.
Lee, K. F., Simon, H., Chen, H., Bates, B., Hung, M. C. and Hauser, C. (1995). Requirement for neuregulin receptor erbB2 in neural and cardiac development. *Nature* **378**, 394-398.
Lee, T. I., Johnstone, S. E. and Young, R. A. (2006). Chromatin immunoprecipitation and microarray-based analysis of protein location. *Nat. Protoc.* **1**, 729-748.
Leimeister, C., Schumacher, N. and Gessler, M. (2003). Expression of Notch pathway genes in the embryonic mouse metanephros suggests a role in proximal tubule development. *Gene Expr. Patterns* **3**, 595-598.
Leung, D. W., Cachianes, G., Kuang, W. J., Goeddel, D. V. and Ferrara, N. (1989). Vascular endothelial growth factor is a secreted angiogenic mitogen. *Science* **246**, 1306-1309.
Levay, A. K., Peacock, J. D., Lu, Y., Koch, M., Hinton, R. B., Jr, Kadler, K. E. and Lincoln, J. (2008). Scleraxis is required for cell lineage differentiation and extracellular matrix remodeling during murine heart valve formation in vivo. *Circ. Res.* **103**, 948-956.
Liu, J., Zhang, L., Wang, D., Shen, H., Jiang, M., Mei, P., Hayden, P. S., Sedor, J. R. and Hu, H. (2003). Congenital diaphragmatic hernia, kidney agenesis and cardiac defects associated with Slit3-deficiency in mice. *Mech. Dev.* **120**, 1059-1070.
Liu, L., Cara, D. C., Kaur, J., Raharjo, E., Mullaly, S. C., Jongstra-Bilen, J., Jongstra, J. and Kubes, P. (2005). LSP1 is an endothelial gatekeeper of leukocyte transendothelial migration. *J. Exp. Med.* **201**, 409-418.
London, T. B., Lee, H. J., Shao, Y. and Zheng, J. (2004). Interaction between the internal motif KTXXXI of Idax and mDvl PDZ domain. *Biochem. Biophys. Res. Commun.* **322**, 326-332.
Luo, G., Hofmann, C., Bronckers, A. L., Sohocki, M., Bradley, A. and Karsenty, G. (1995). BMP-7 is an inducer of nephrogenesis, and is also required for eye development and skeletal patterning. *Genes Dev.* **9**, 2808-2820.
Lyons, K. M., Hogan, B. L. and Robertson, E. J. (1995). Colocalization of BMP 7 and BMP 2 RNAs suggests that these factors cooperatively mediate tissue interactions during murine development. *Mech. Dev.* **50**, 71-83.
Macisaac, K. D., Gordon, D. B., Nekludova, L., Odom, D. T., Schreiber, J., Gifford, D. K., Young, R. A. and Fraenkel, E. (2006). A hypothesis-based approach for identifying the binding specificity of regulatory proteins from chromatin immunoprecipitation data. *Bioinformatics* **22**, 423-429.
Marion, R. M., Fortes, P., Beloso, A., Dotti, C. and Ortin, J. (1999). A human sequence homologue of Staufen is an RNA-binding protein that is associated with polysomes and localizes to the rough endoplasmic reticulum. *Mol. Cell. Biol.* **19**, 2212-2219.
Matsunaga, E. (1981). Genetics of Wilms' tumor. *Hum. Genet.* **57**, 231-246.
Meagher, M. J. and Braun, R. E. (2001). Requirement for the murine zinc finger protein ZFR in perigastrulation growth and survival. *Mol. Cell. Biol.* **21,** 2880-2890.
Miller, S. F., Summerhurst, K., Runker, A. E., Kerjan, G., Friedel, R. H., Chedotal, A., Murphy, P. and Mitchell, K. J. (2007). Expression of Plxdc2/TEM7R in the developing nervous system of the mouse. *Gene Expr. Patterns* **7**, 635-644.
Mitiku, N. and Baker, J. C. (2007). Genomic analysis of gastrulation and organogenesis in the mouse. *Dev. Cell* **13**, 897-907.
Miyazaki, Y., Oshima, K., Fogo, A., Hogan, B. L. and Ichikawa, I. (2000). Bone morphogenetic protein 4 regulates the budding site and elongation of the mouse ureter. *J. Clin. Invest.* **105**, 863-873.
Mo, R., Freer, A. M., Zinyk, D. L., Crackower, M. A., Michaud, J., Heng, H. H., Chik, K. W., Shi, X. M., Tsui, L. C., Cheng, S. H. et al. (1997). Specific and redundant functions of Gli2 and Gli3 zinc finger genes in skeletal patterning and development. *Development* **124**, 113-123.
Moore, A. W., Schedl, A., McInnes, L., Doyle, M., Hecksher-Sorensen, J. and Hastie, N. D. (1998). YAC transgenic analysis reveals Wilms' tumour 1 gene activity in the proliferating coelomic epithelium, developing diaphragm and limb. *Mech. Dev.* **79**, 169-184.
Moore, A. W., McInnes, L., Kreidberg, J., Hastie, N. D. and Schedl, A. (1999). YAC complementation shows a requirement for Wt1 in the development of epicardium, adrenal gland and throughout nephrogenesis. *Development* **126**, 1845-1857.
Muir, T., Sadler-Riggleman, I. and Skinner, M. K. (2005). Role of the basic helix-loop-helix transcription factor, scleraxis, in the regulation of Sertoli cell function and differentiation. *Mol. Endocrinol.* **19**, 2164-2174.
Mundlos, S., Pelletier, J., Darveau, A., Bachmann, M., Winterpacht, A. and Zabel, B. (1993). Nuclear localization of the protein encoded by the Wilms' tumor gene WT1 in embryonic and adult tissues. *Development* **119**, 1329-1341.
Murone, M., Rosenthal, A. and de Sauvage, F. J. (1999). Sonic hedgehog signaling by the patched-smoothened receptor complex. *Curr. Biol.* **9**, 76-84.
Nakagama, H., Heinrich, G., Pelletier, J. and Housman, D. E. (1995). Sequence and structural requirements for high-affinity DNA binding by the WT1 gene product. *Mol. Cell. Biol.* **15**, 1489-1498.
Nakao, A., Afrakhte, M., Moren, A., Nakayama, T., Christian, J. L., Heuchel, R., Itoh, S., Kawabata, M., Heldin, N. E., Heldin, C. H. et al. (1997). Identification of Smad7, a TGFbeta-inducible antagonist of TGF-beta signalling. *Nature* **389**, 631-635.
Nishinakamura, R., Matsumoto, Y., Nakao, K., Nakamura, K., Sato, A., Copeland, N. G., Gilbert, D. J., Jenkins, N. A., Scully, S., Lacey, D. L. et al. (2001). Murine homolog of SALL1 is essential for ureteric bud invasion in kidney development. *Development* **128**, 3105-3115.
Pal, C. and Hurst, L. D. (2000). The evolution of gene number: are heritable and non-heritable errors equally important? *Heredity* **84**, 393-400.
Pavletich, N. P. and Pabo, C. O. (1993). Crystal structure of a five-finger GLI-DNA complex: new perspectives on zinc fingers. *Science* **261,** 1701-1707.
Pelletier, J., Schalling, M., Buckler, A. J., Rogers, A., Haber, D. A. and Housman, D. (1991). Expression of the Wilms' tumor gene WT1 in the murine urogenital system. *Genes Dev.* **5**, 1345-1356.
Pendino, F., Nguyen, E., Jonassen, I., Dysvik, B., Azouz, A., Lanotte, M., Segal-Bendirdjian, E. and Lillehaug, J. R. (2009). Functional involvement of RINF, retinoid-inducible nuclear factor (CXXC5), in normal and tumoral human myelopoiesis. *Blood* **113**, 3172-3181.
Piscione, T. D., Phan, T. and Rosenblum, N. D. (2001). BMP7 controls collecting tubule cell proliferation and apoptosis via Smad1-dependent and -independent pathways. *Am. J. Physiol. Renal Physiol.* **280**, F19-F33.
Poladia, D. P., Kish, K., Kutay, B., Hains, D., Kegg, H., Zhao, H. and Bates, C. M. (2006). Role of fibroblast growth factor receptors 1 and 2 in the metanephric mesenchyme. *Dev. Biol.* **291**, 325-339.
Pritchard-Jones, K., Fleming, S., Davidson, D., Bickmore, W., Porteous, D., Gosden, C., Bard, J., Buckler, A., Pelletier, J., Housman, D. et al. (1990). The

candidate Wilms' tumour gene is involved in genitourinary development. *Nature* **346**, 194-197.
Rauscher, F. J., 3rd, Morris, J. F., Tournay, O. E., Cook, D. M. and Curran, T. (1990). Binding of the Wilms' tumor locus zinc finger protein to the EGR-1 consensus sequence. *Science* **250**, 1259-1262.
Reddy, J. C., Hosono, S. and Licht, J. D. (1995). The transcriptional effect of WT1 is modulated by choice of expression vector. *J. Biol. Chem.* **270**, 29976-29982.
Rothenpieler, U. W. and Dressler, G. R. (1993). Pax-2 is required for mesenchyme-to-epithelium conversion during kidney development. *Development* **119**, 711-720.
Ryan, G., Steele-Perkins, V., Morris, J. F., Rauscher, F. J., 3rd and Dressler, G. R. (1995). Repression of Pax-2 by WT1 during normal kidney development. *Development* **121**, 867-875.
Scharnhorst, V., van der Eb, A. J. and Jochemsen, A. G. (2001). WT1 proteins: functions in growth and differentiation. *Gene* **273**, 141-161.
Schnabel, C. A., Godin, R. E. and Cleary, M. L. (2003). Pbx1 regulates nephrogenesis and ureteric branching in the developing kidney. *Dev. Biol.* **254**, 262-276.
Scholz, H., Wagner, K. D. and Wagner, N. (2009). Role of the Wilms' tumour transcription factor, Wt1, in blood vessel formation. *Pflugers Arch.* **458**, 315-323.
Schwabe, J. W., Fairall, L., Chapman, L., Finch, J. T., Dutnall, R. N. and Rhodes, D. (1993). The cocrystal structures of two zinc-stabilized DNA-binding domains illustrate different ways of achieving sequence-specific DNA recognition. *Cold Spring Harb. Symp. Quant. Biol.* **58,** 141-147.
Self, M., Lagutin, O. V., Bowling, B., Hendrix, J., Cai, Y., Dressler, G. R. and Oliver, G. (2006). Six2 is required for suppression of nephrogenesis and progenitor renewal in the developing kidney. *EMBO J.* **25**, 5214-5228.
Sock, E., Rettig, S. D., Enderich, J., Bosl, M. R., Tamm, E. R. and Wegner, M. (2004). Gene targeting reveals a widespread role for the high-mobility-group transcription factor Sox11 in tissue remodeling. *Mol. Cell. Biol.* **24**, 6635-6644.
Steidl, C., Leimeister, C., Klamt, B., Maier, M., Nanda, I., Dixon, M., Clarke, R., Schmid, M. and Gessler, M. (2000). Characterization of the human and mouse HEY1, HEY2, and HEYL genes: cloning, mapping, and mutation screening of a new bHLH gene family. *Genomics* **66**, 195-203.
Stone, D. M., Hynes, M., Armanini, M., Swanson, T. A., Gu, Q., Johnson, R. L., Scott, M. P., Pennica, D., Goddard, A., Phillips, H. et al. (1996). The tumour-suppressor gene patched encodes a candidate receptor for Sonic hedgehog. *Nature* **384**, 129-134.
Taketomi, T., Yoshiga, D., Taniguchi, K., Kobayashi, T., Nonami, A., Kato, R., Sasaki, M., Sasaki, A., Ishibashi, H., Moriyama, M. et al. (2005). Loss of mammalian Sprouty2 leads to enteric neuronal hyperplasia and esophageal achalasia. *Nat. Neurosci.* **8**, 855-857.
Tang, X., Feng, Y. and Ye, K. (2007). Src-family tyrosine kinase fyn phosphorylates phosphatidylinositol 3-kinase enhancer-activating Akt, preventing its apoptotic cleavage and promoting cell survival. *Cell Death Differ.* **14**, 368-377.
Taniguchi, K., Ayada, T., Ichiyama, K., Kohno, R., Yonemitsu, Y., Minami, Y., Kikuchi, A., Maehara, Y. and Yoshimura, A. (2007). Sprouty2 and Sprouty4 are essential for embryonic morphogenesis and regulation of FGF signaling. *Biochem. Biophys. Res. Commun.* **352**, 896-902.
Thate, C., Englert, C. and Gessler, M. (1998). Analysis of WT1 target gene expression in stably transfected cell lines. *Oncogene* **17**, 1287-1294.
Torres, M., Gomez-Pardo, E. and Gruss, P. (1996). Pax2 contributes to inner ear patterning and optic nerve trajectory. *Development* **122**, 3381-3391.
Toyofuku, T., Zhang, H., Kumanogoh, A., Takegahara, N., Suto, F., Kamei, J., Aoki, K., Yabuki, M., Hori, M., Fujisawa, H. et al. (2004a). Dual roles of Sema6D in cardiac morphogenesis through region-specific association of its receptor, Plexin-A1, with off-track and vascular endothelial growth factor receptor type 2. *Genes Dev.* **18**, 435-447.
Toyofuku, T., Zhang, H., Kumanogoh, A., Takegahara, N., Yabuki, M., Harada, K., Hori, M. and Kikutani, H. (2004b). Guidance of myocardial patterning in cardiac development by Sema6D reverse signalling. *Nat. Cell Biol.* **6**, 1204-1211.
Vokes, S. A., Ji, H., McCuine, S., Tenzen, T., Giles, S., Zhong, S., Longabaugh, W. J., Davidson, E. H., Wong, W. H. and McMahon, A. P. (2007). Genomic characterization of Gli-activator targets in sonic hedgehog-mediated neural patterning. *Development* **134**, 1977-1989.
Wagner, K. D., Wagner, N., Vidal, V. P., Schley, G., Wilhelm, D., Schedl, A., Englert, C. and Scholz, H. (2002). The Wilms' tumor gene Wt1 is required for normal development of the retina. *EMBO J.* **21**, 1398-1405.
Wagner, N., Wagner, K. D., Hammes, A., Kirschner, K. M., Vidal, V. P., Schedl, A. and Scholz, H. (2005). A splice variant of the Wilms' tumour suppressor Wt1 is required for normal development of the olfactory system. *Development* **132**, 1327-1336.
Watson, A. J. and Barcroft, L. C. (2001). Regulation of blastocyst formation. *Front. Biosci.* **6**, D708-D730.
Wellik, D. M. (2009). Hox genes and vertebrate axial pattern. *Curr. Top. Dev. Biol.* **88**, 257-278.
Wu, R. Y., Zhang, Y., Feng, X. H. and Derynck, R. (1997). Heteromeric and homomeric interactions correlate with signaling activity and functional cooperativity of Smad3 and Smad4/DPC4. *Mol. Cell. Biol.* **17**, 2521-2528.
Wurm, A., Sock, E., Fuchshofer, R., Wegner, M. and Tamm, E. R. (2008). Anterior segment dysgenesis in the eyes of mice deficient for the high-mobility-group transcription factor Sox11. *Exp. Eye Res.* **86**, 895-907.
Xu, X., Weinstein, M., Li, C., Naski, M., Cohen, R. I., Ornitz, D. M., Leder, P. and Deng, C. (1998). Fibroblast growth factor receptor 2 (FGFR2)-mediated reciprocal regulation loop between FGF8 and FGF10 is essential for limb induction. *Development* **125**, 753-765.
Zhang, X., Xing, G. and Saunders, G. F. (1999). Proto-oncogene N-myc promoter is down regulated by the Wilms' tumor suppressor gene WT1. *Anticancer Res.* **19**, 1641-1648.
Zhang, Y., Feng, X., We, R. and Derynck, R. (1996). Receptor-associated Mad homologues synergize as effectors of the TGF-beta response. *Nature* **383**, 168-172.
Zhao, H., Kegg, H., Grady, S., Truong, H. T., Robinson, M. L., Baum, M. and Bates, C. M. (2004). Role of fibroblast growth factor receptors 1 and 2 in the ureteric bud. *Dev. Biol.* **276**, 403-415.